Supporting Information: Multiconfiguration Pair-Density Functional Theory for Chromium(IV) Molecular Qubits

Arturo Sauza-de la Vega,[†] Riddhish Pandharkar,[†,¶] Gautam D. Stroscio,[†] Arup Sarkar,[†] Donald G. Truhlar,[*,‡] and Laura Gagliardi[*,†,¶]

†*Department of Chemistry, Pritzker School of Molecular Engineering, James Franck Institute, Chicago Center for Theoretical Chemistry, University of Chicago, Chicago, Illinois 60637, United States*

‡*Department of Chemistry, Chemical Theory Center, and Minnesota Supercomputing Institute, University of Minnesota, Minneapolis, Minnesota 55455–0431, United States*

¶*Argonne National Laboratory, Lemont, Illinois 60439, United States*

E-mail: truhlar@umn.edu; lgagliardi@uchicago.edu

Contents

Date of finalization: August 15, 2022

1 Computational details of Kohn-Sham density functional calculations

Kohn-Sham density functional calculations were performed using ORCA[S1,S2] version 5.0.

For the desnity functional calculations, we used the B3LYP,[S3–S6] BP86,[S3,S7] M06-L,[S8,S9] M06,[S9] M06-2X,[S9] TPSS,[S10–S12] PBE,[S13] PBE0,[S14,S15] and ωB97X[S16] exchange-correlation functionals to calculate the axial (D) and rhombic (E) zero field splitting parameters (see example input file in Section S1) using the VASP-optimized geometry of complexes **1**, **2**, and

3. The def2-TZVP basis set[S17] was used on all atoms. For the local exchange-correlation functionals, we used Split-RI-J, which is the default and recommended version of the resolution of identity[S18–S23] approximation. For the hybrid exchange-correlation functionals, the RIJCOSX[S19] approximation was used. Tight SCF convergence criteria were applied for all these density functional calculations. The coupled-perturbed method[S24] was used for the spin-orbit coupling contribution to the D-tensor. Calculations were performed with both spin-orbit coupling and spin-spin coupling and with only spin-orbit coupling (Tables S1-S3 and Figures S1-S2).

1.1 Examples of ORCA input files (excluding coordinates)

Example using the BP86 functional

```
!  UKS BP86 def2-TZVP RI def2/J decontractauxj TIGHTSCF
! SlowConv LargePrint PrintBasis MOREAD
%moinp "Cr_Toluene_VASP-BP86-DTensor.gbw"

%pal
nprocs 16
end
%maxcore 3000

%eprnmr
DTensor ssandso
DSOC cp
DSS uno
end

*xyz 0 3
```

Example using the B3LYP functional

```
!  UKS B3LYP def2-TZVP RIJCOSX def2/J decontractauxj TIGHTSCF
! SlowConv LargePrint PrintBasis MOREAD
%moinp "Cr_Toluene_VASP-B3LYP-DTensor.gbw"

%pal
nprocs 16
end
%maxcore 3000

%eprnmr
DTensor ssandso
DSOC cp
DSS uno
end

*xyz 0 3
```

Example of SA-CASSCF/NEVPT2 calculation

```
!  DKH2 DKH-def2-TZVP RIJCOSX def2/j def2-tzvp/c decontractauxj decontractauxc
!  LargePrint PrintBasis MOREAD
%moinp "Cr-Toluene-VASP-2in5-NEV_decontractauxc.gbw"

%casscf
nel 2
norb 5
```

```
mult 3,1
nroots 10,15
printwf det
trafostep ri
ptmethod sc_nevpt2
rel
dosoc true
dossc true
gtensor true
end
end

%pal
nprocs 16
end
%maxcore 3000

*xyz 0 3
```

1.2 Examples of OpenMolcas input files (excluding coordinates)

```
 &GATEWAY
RICD
COORD = Cr_Toluene_opt.xyz
group = nosym
basis = Cr.ANO-RCC-VTZP, C.ANO-RCC-VDZ, H.ANO-RCC-VDZ
End of Input
```

```
&SEWARD
End Of Input

>>COPY $CurrDir/cas2-5_tol_opt_triplet.RasOrb INPORB

&RASSCF
Lumorb
Symmetry = 1
Spin = 3
NACTEL = 2 0 0
CHARGE = 0
RAS2 = 5
CIROOT = 10 10 1
ORBListing
ALL
ORBAppear
COMPACT
ITERations = 200 100; CIMX = 500
Sdav = 200; PRWF = 0.01
End of Input

>>COPY $WorkDir/$Project.RasOrb $CurrDir/$Project.RasOrb
>>COPY $CurrDir/$Project.RasOrb INPORB

&MCPDFT
KSDFT = tPBE
```

```
NOGRADIENT


&CASPT2

NoMult

MULTistate

10 1 2 3 4 5 6 7 8 9 10

Imag = 0.3

MAXIter = 100

IPEA = 0.25

End Of Input
```

1.3 Energy gaps by Kohn-Sham density functional theory

Table S1: Calculated triplet-singlet gaps using the optimized **1** structure by Kohn–Sham density functional calculations with various exchange-correlation functionals

	$\Delta E_{\text{T-S}}$ (eV)	$\Delta E_{\text{T-S}}$ (cm^{-1})*
B3LYP	1.64	13 216.7
BP86	1.46	11 759.7
M06	1.93	15 557.8
M06-2X	1.86	14 993.3
M06-L	1.81	14 578.7
PBE	1.45	11 728.8
PBE0	1.83	14 744.3
TPSS	1.52	12 259.2
ωB97X	1.71	13 792.1
Experiment	1.20	9 678.6

*1 eV = 8 065.54 cm^{-1}.

Table S2: Calculated triplet-singlet gaps using the optimized **2** structure by Kohn–Sham density functional calculations with various exchange-correlation functionals

	$\Delta E_{\text{T-S}}$ (eV)	$\Delta E_{\text{T-S}}$ (cm^{-1})*
B3LYP	1.73	13 918.2
BP86	1.48	11 955.5
M06	1.93	15 586.1
M06-2X	1.98	15 966.5
M06-L	1.81	14 596.1
PBE	1.48	11 900.0
PBE0	1.92	15 466.8
TPSS	1.56	12 571.7
ωB97X	1.81	14 627.4
Experiment	1.22	9 839.9

*1 eV = 8 065.54 cm^{-1}.

Table S3: Calculated triplet-singlet gaps using the optimized **3** structure by Kohn–Sham density functional calculations with various exchange-correlation functionals

	$\Delta E_{\text{T-S}}$ (eV)	$\Delta E_{\text{T-S}}$ (cm^{-1})*
B3LYP	1.74	13 999.4
BP86	1.43	11 503.5
M06	1.80	14 553.8
M06-2X	2.01	16 175.7
M06-L	1.79	14 406.3
PBE	1.42	11 423.4
PBE0	1.93	15 565.0
TPSS	1.51	12 216.6
ωB97X	1.84	14 849.7
Experiment	1.20	9 678.6

*1 eV = 8 065.54 cm^{-1}.

1.4 Zero-field splitting parameters by Kohn-Sham density functional theory

Table S4: Calculated absolute values (in GHz) for the axial (D) and rhombic (E) zero-field splitting parameters by Kohn–Sham density functional calculations at the VASP-optimized **1** structure

	|D| (GHz)	|E| (GHz)	$\|D\|$ (cm^{-1})	$\|E\|$ (cm^{-1})
B3LYP	5.49	0.05	0.183	0.002
BP86	7.03	0.00	0.234	0.000
M06	4.08	0.04	0.136	0.001
M06-2X	4.08	0.07	0.136	0.002
M06-L	2.42	0.00	0.081	0.000
PBE	7.22	0.01	0.241	0.000
PBE0	5.09	0.07	0.170	0.002
TPSS	5.96	0.07	0.199	0.002
ωB97X	5.27	0.50	0.176	0.017
Experiment	3.53	0.00	0.118	0.000

* 1 cm^{-1} = 29.9792 GHz.

Table S5: Calculated absolute values (in GHz) for the axial (D) and rhombic (E) zero-field splitting parameters by Kohn–Sham density functional calculations at the VASP-optimized **2** structure

	|D| (GHz)	|E| (GHz)	$\|D\|$ (cm^{-1})	$\|E\|$ (cm^{-1})
B3LYP	3.19	0.52	0.106	0.017
BP86	4.74	0.49	0.158	0.016
M06	2.50	0.13	0.083	0.004
M06-2X	1.88	0.15	0.063	0.005
M06-L	3.36	0.36	0.112	0.012
PBE	4.91	0.39	0.164	0.013
PBE0	2.73	0.49	0.091	0.016
TPSS	4.31	0.38	0.144	0.013
ωB97X	2.24	0.51	0.075	0.017
Experiment	1.92	0.53	0.064	0.018

* 1 cm^{-1} = 29.9792 GHz.

Table S6: Calculated absolute values (in GHz) for the axial (D) and rhombic (E) zero-field splitting parameters by Kohn–Sham density functional calculations at the VASP-optimized **3** structure

	|D| (GHz)	|E| (GHz)	$\|D\|$ (cm^{-1})	$\|E\|$ (cm^{-1})
B3LYP	1.14	0.06	0.038	0.002
BP86	2.52	0.09	0.084	0.003
M06	4.11	0.21	0.137	0.007
M06-2X	4.14	0.30	0.138	0.010
M06-L	1.23	0.11	0.041	0.004
PBE	2.38	0.07	0.079	0.002
PBE0	0.73	0.01	0.024	0.000
TPSS	2.30	0.10	0.077	0.003
ωB97X	0.76	0.05	0.025	0.002
Experiment	4.19	0.48	0.140	0.016

* 1 cm^{-1} = 29.9792 GHz.

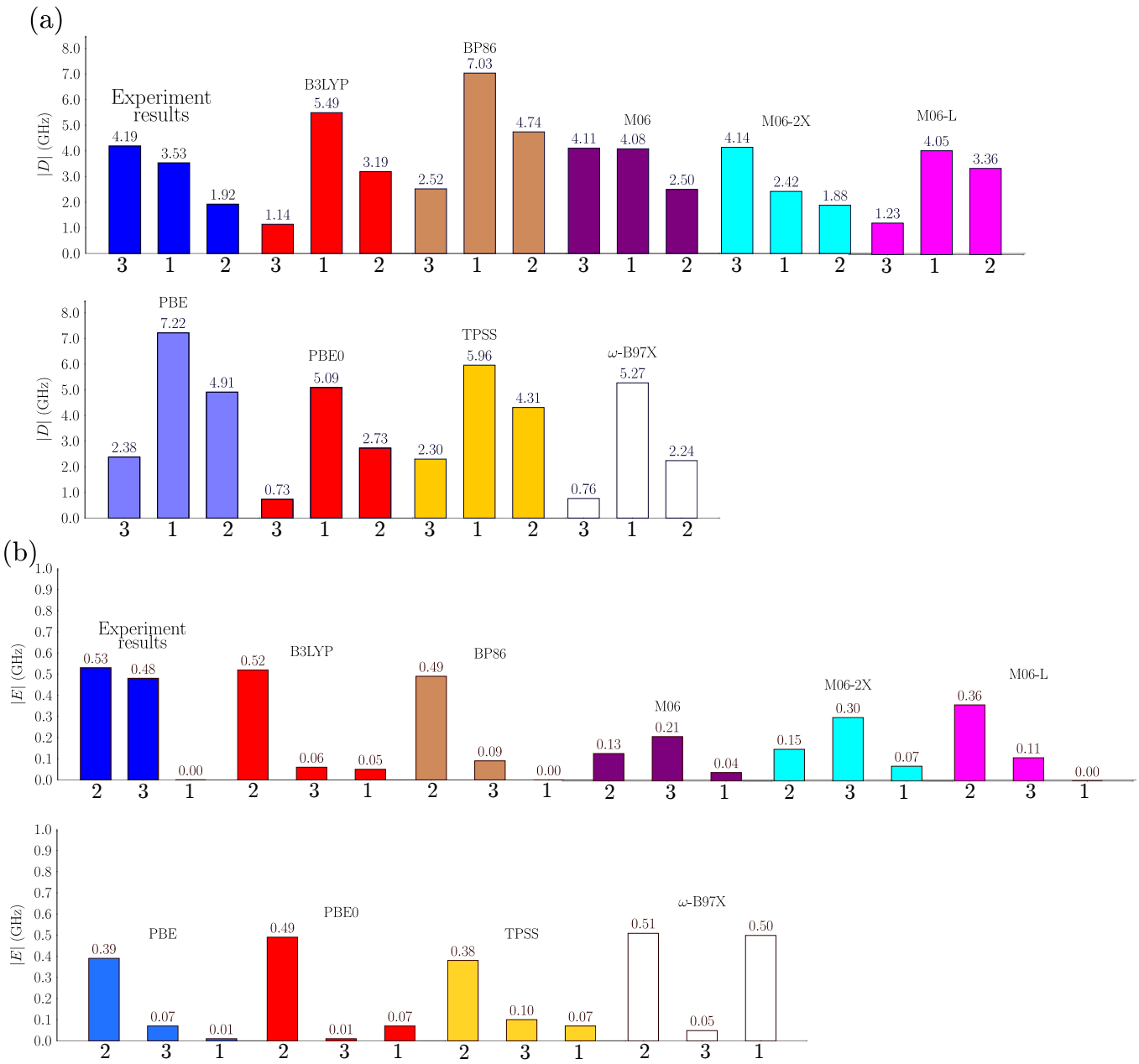

Figure S1: Experimental and calculated values (in GHz) of (a) the axial parameter $|D|$, (b) the rhombic parameter $|E|$. The blue bars are the experimental findings, and the other bars are the computational data using the VASP optimized structure and the B3LYP, BP86, M06, M06-2X, M06-L, PBE, PBE0, TPSS, and ω-B97X exchange-correlation functionals in Kohn-Sham density functional calculations with the def2-TZVP basis set.

1.5 Zero-field splitting by by ORCA SA-CASSCF and NEVPT2 calculations

Table S7: Absolute values (in GHz) for the axial zero-field splitting parameter (D) calculated with SA-CASSCF and NEVPT2, for the experimental and optimized geometries.

	Experimental structure				
	SA-CASSCF	SA-CASSCF*	NEVPT2	NEVPT2*	Experiment
1	9.93	10.00	5.37	5.53	3.53
2	2.74	3.14	4.46	4.48	1.92
3	5.12	5.23	1.96	2.11	4.19
	VASP optimized structure				
	SA-CASSCF	SA-CASSCF*	NEVPT2	NEVPT2*	Experiment
1	10.65	10.73	3.06	3.18	3.53
2	1.08	1.22	0.48	0.64	1.92
3	4.14	4.23	0.77	0.86	4.19

* Indicates that in addition to spin-orbit coupling, spin-spin coupling was included in the calculation.

Table S8: Absolute values (in GHz) for the rhombic zero-field splitting parameter (E) calculated with SA-CASSCF and NEVPT2, for the experimental and optimized geometries.

	Experimental structure				
	SA-CASSCF	SA-CASSCF*	NEVPT2	NEVPT2*	Experiment
1	0.28	0.70	1.43	1.83	0.00
2	0.37	0.46	0.65	0.92	0.53
3	0.82	0.86	0.13	0.16	0.48
	VASP optimized structure				
	SA-CASSCF	SA-CASSCF*	NEVPT2	NEVPT2*	Experiment
1	0.01	0.01	0.01	0.01	0.00
2	0.32	0.34	0.13	0.18	0.53
3	1.02	1.06	0.21	0.22	0.48

* Indicates that in addition to spin-orbit coupling, spin-spin coupling was included in the calculation.

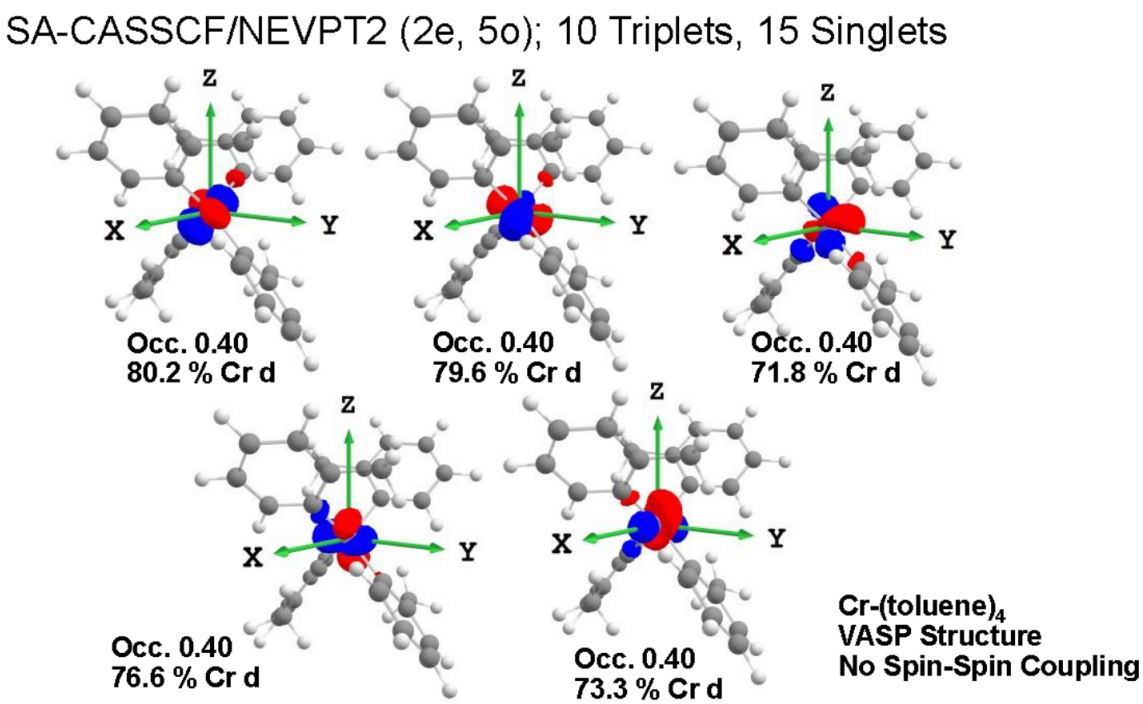

Figure S2: Representative active orbitals used in SA-CASSCF(2,5)/NEVPT2 calculations.

2 Structures

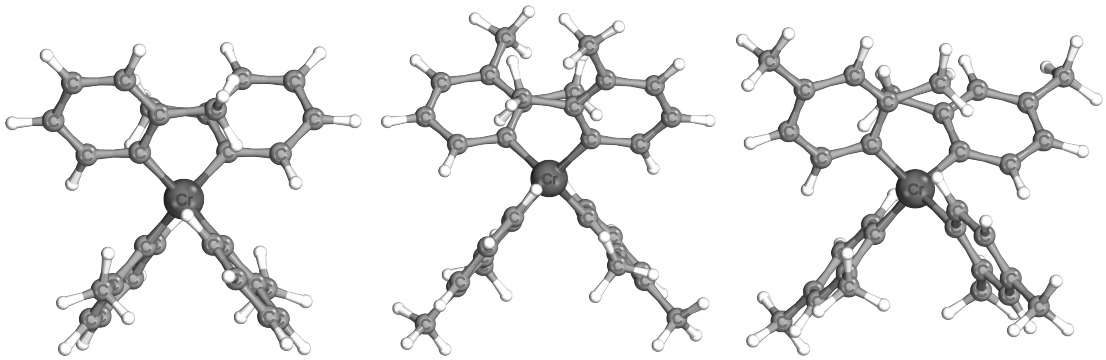

(a) **1** (b) **2** (c) **3**

Figure S3: Molecular structures of the optimized Cr(IV) aryl complexes studied in this article.

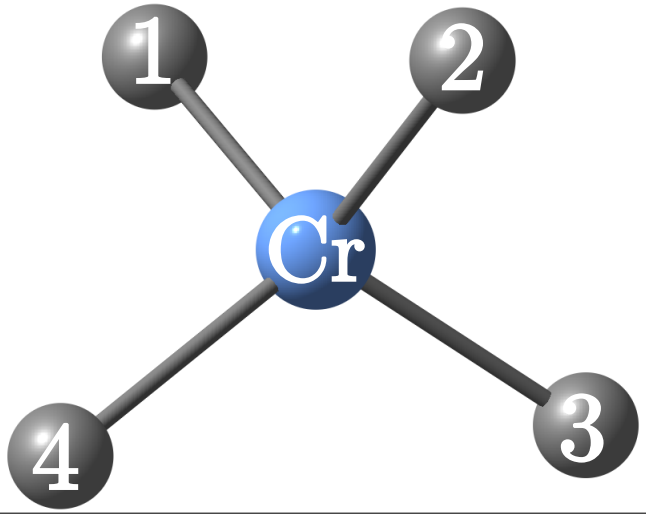

Bond distances			
Atoms	Unit Cell Opt. Geom. (Å)	Expt. Geom. (Å)	Gas-Phase Opt. Geom. (Å)
Cr-1	1.97	2.00	1.98
Cr-2	1.97	1.99	1.98
Cr-3	1.97	1.98	1.98
Cr-4	1.97	1.99	1.98
Bond angles			
Atoms	Unit Cell Opt. Geom. (deg)	Expt. Geom. (deg)	Gas-Phase Opt. Geom. (deg)
1-Cr-2	102.4	102.4	104.8
1-Cr-3	113.2	113.5	111.8
1-Cr-4	113.2	110.9	111.8
2-Cr-3	113.2	111.9	111.8
2-Cr-4	113.2	113.3	111.9
3-Cr-4	102.3	105.1	104.8

Figure S4: Geometrical data for molecule **1** optimized and experimental structures.

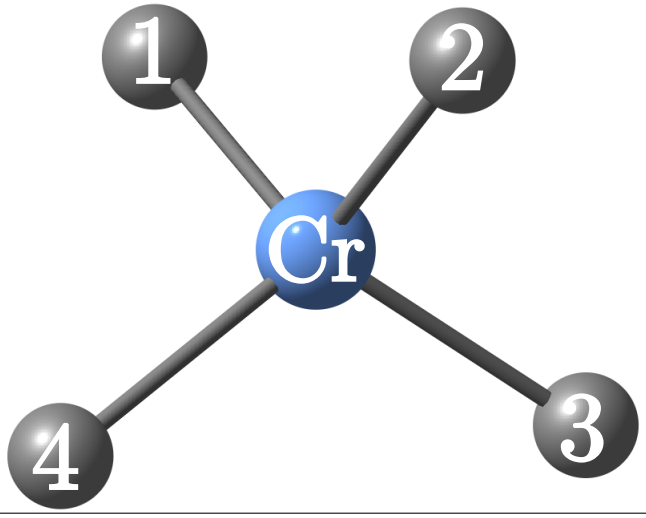

Bond distances			
Atoms	Unit Cell Opt. Geom. (Å)	Expt. Geom. (Å)	Gas-Phase Opt. Geom. (Å)
Cr-1	1.98	2.02	1.98
Cr-2	1.98	2.02	1.98
Cr-3	1.98	2.00	1.98
Cr-4	1.98	2.00	1.98
Bond angles			
Atoms	Unit Cell Opt. Geom. (deg)	Expt. Geom. (deg)	Gas-Phase Opt. Geom. (deg)
1-Cr-2	107.9	107.8	104.5
1-Cr-3	110.4	110.4	111.9
1-Cr-4	109.5	109.6	112.0
2-Cr-3	109.5	109.6	111.9
2-Cr-4	110.4	110.4	112.0
3-Cr-4	109.2	109.2	104.5

Figure S5: Geometrical data for molecule **2** optimized and experimental structures.

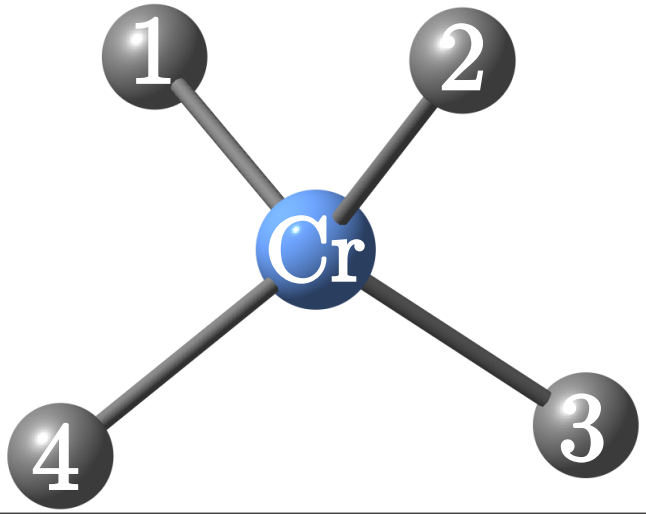

Bond distances			
Atoms	Unit Cell Opt. Geom. (Å)	Expt. Geom. (Å)	Gas-Phase Opt. Geom. (Å)
Cr-1	1.98	2.00	1.98
Cr-2	1.98	1.99	1.98
Cr-3	1.97	2.00	1.97
Cr-4	1.97	1.99	1.97
Bond angles			
Atoms	Unit Cell Opt. Geom. (deg)	Expt. Geom. (deg)	Gas-Phase Opt. Geom. (deg)
1-Cr-2	109.1	109.3	104.3
1-Cr-3	109.2	109.1	111.8
1-Cr-4	109.7	110.6	112.0
2-Cr-3	111.1	109.7	112.5
2-Cr-4	109.3	109.1	112.3
3-Cr-4	108.5	109.0	104.2

Figure S6: Geometrical data for molecule **3** optimized and experimental structures.

3 Active spaces

In the following figures are shown the molecular orbitals used for each of the complexes in each active space.

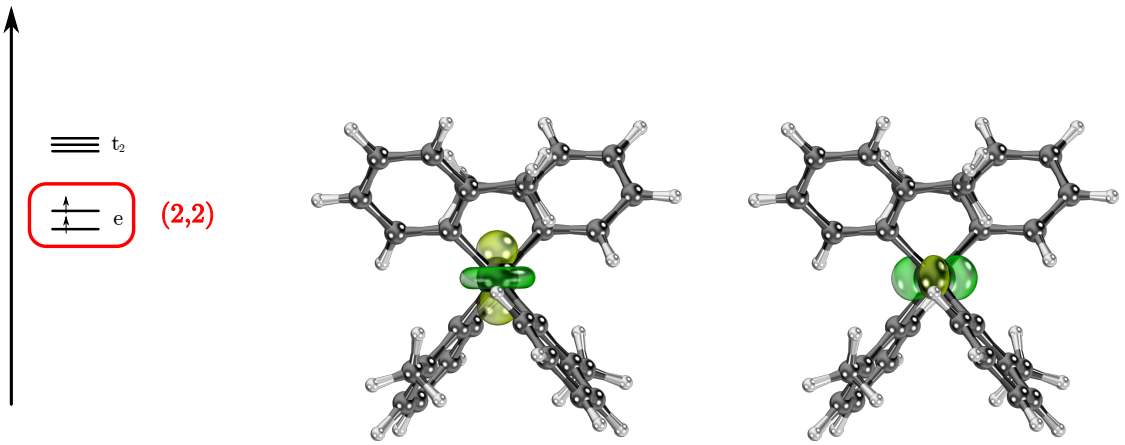

Figure S7: Molecular orbitals in the (2,2) active space of complex **1**.

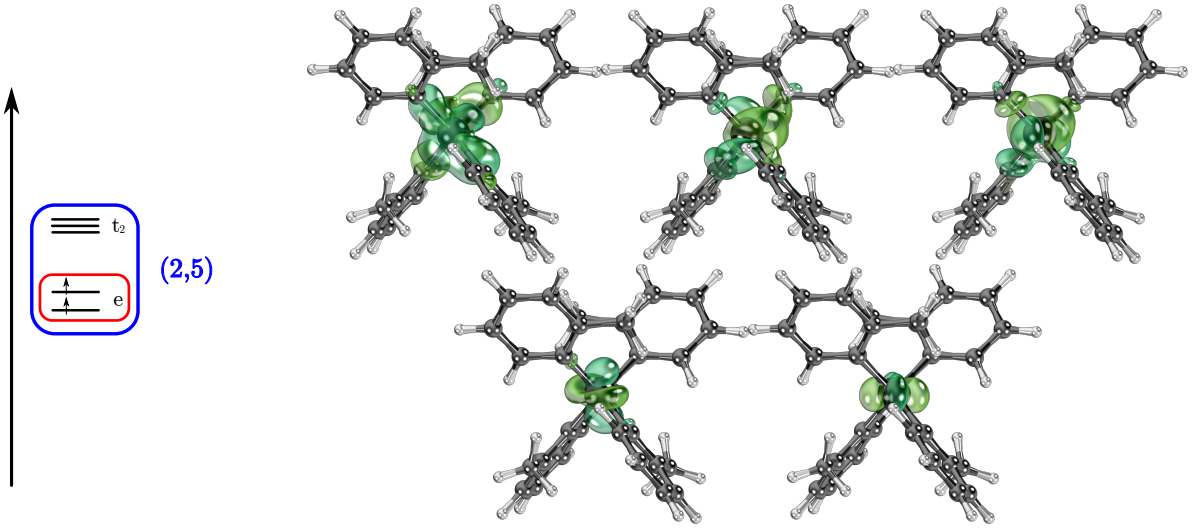

Figure S8: Molecular orbitals in the (2,5) active space of complex **1**.

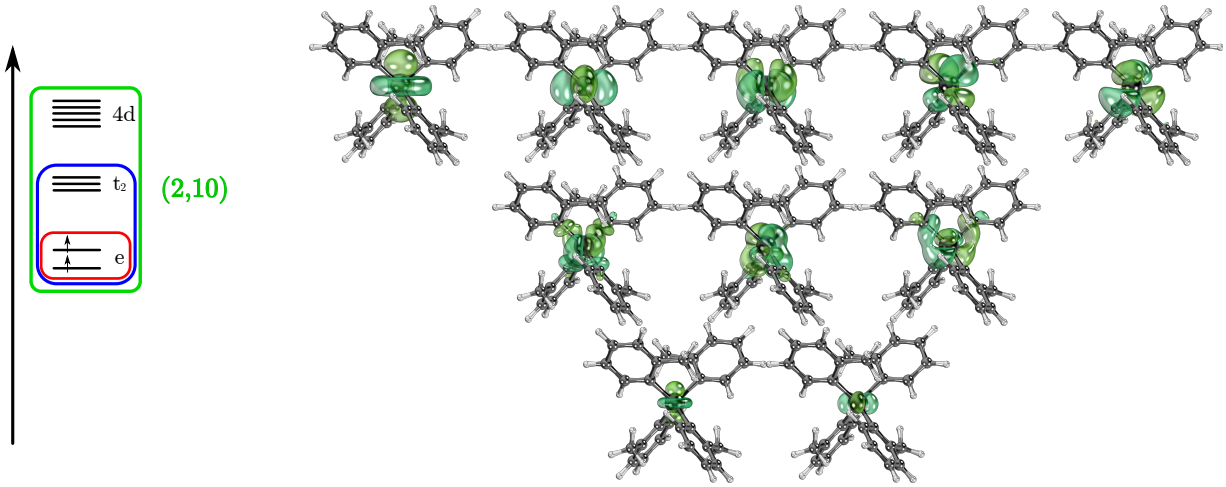

Figure S9: Molecular orbitals in the (2,10) active space of complex **1**.

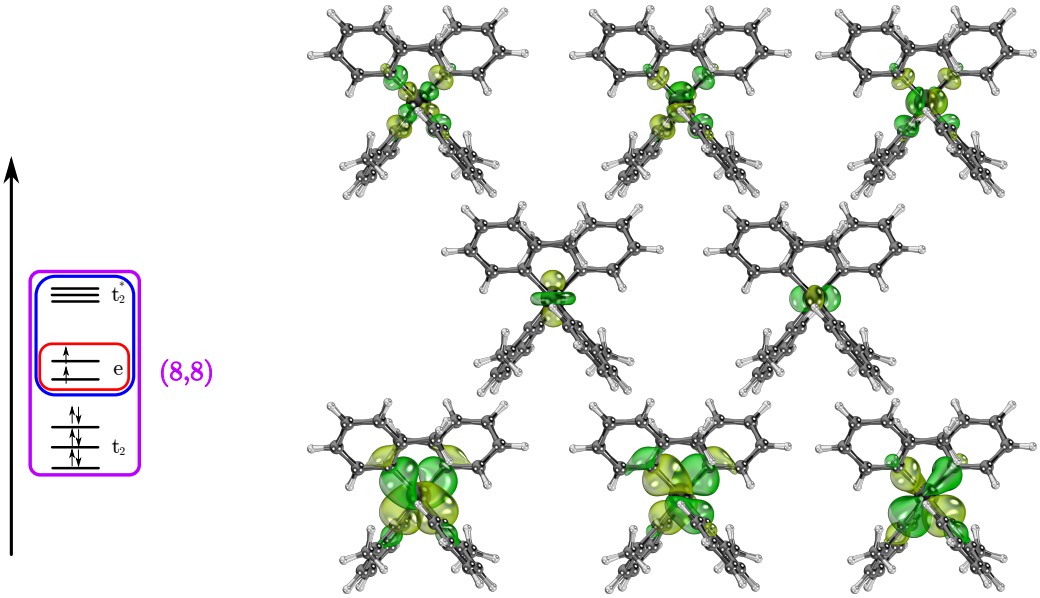

Figure S10: Molecular orbitals in the (8,8) active space of complex **1**.

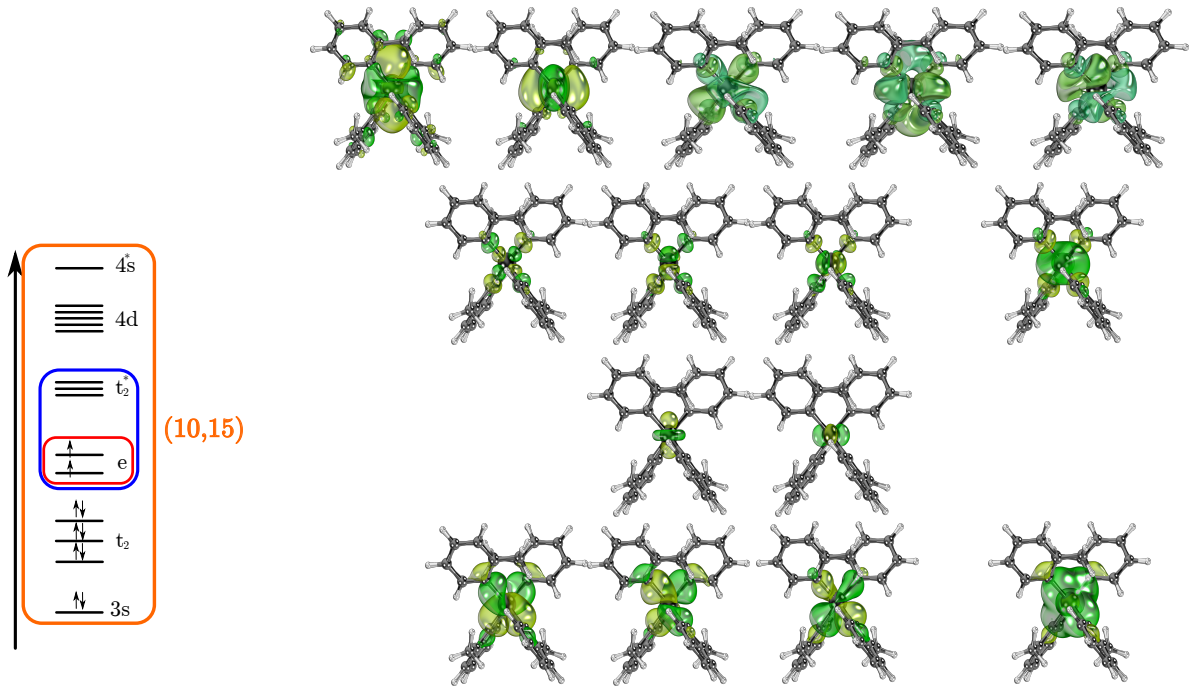

Figure S11: Molecular orbitals in the (10,15) active space of complex **1**.

4 Energy gaps ($\Delta E_{\text{T-S}}$)

The energy difference between the triplet ground-state and the first excited state (a singlet) for the chromium(IV) complexes using the five active spaces considered in this research are given in the following tables.

Table S9: Calculated triplet-singlet gaps ($\Delta E_{\text{T-S}}$) in eV and cm^{-1} inside the parenthesis, using the unit cell optimized triplet structure of molecule **1**, the experimental structure, and gas-pahse optimized triplet and singlet structures. The energy gaps were obtained with SA-CASSCF, MS-CASPT2, tPBE and tPBE0 methods.

Periodic optimized geometry					
Active space	SA-CASSCF	MS-CASPT2	tPBE	tPBE0	Expt.
(2, 2)	1.87(14 254.7)	1.23(9 778.6)	0.55(5 110.2)	0.88(7 396.3)	
(2, 5)	1.89(15 218.6)	0.94(7 606.5)	0.48(3 831.2)	0.83(6 678.1)	
(2, 10)	1.81(14 634.1)	0.98(7 902.4)	0.51(4 096.8)	0.83(6 731.1)	
(8, 8)	1.83(15 561.1)	1.41(11 592.9)	0.94(7 407.4)	1.16(9 445.8)	
(10, 15)	1.66(13 388.8)	1.41(11 353.5)	1.02(8 226.9)	1.18(9 517.3)	1.20(9 678.6)
Experimental geometry					
Active space	SA-CASSCF	MS-CASPT2	tPBE	tPBE0	Expt.
(2,2)	1.75(14 105.3)	1.20(9 697.0)	0.64(5 201.2)	0.92(7 427.2)	
(2,5)	1.89(15 212.6)	0.92(7 418.6)	0.49(3 927.5)	0.84(6 748.8)	
(2,10)	1.81(14 620.7)	0.97(7 800.1)	0.52(4 174.4)	0.98(7 882.2)	
(8,8)	1.83(14 740.9)	1.43(11 565.9)	0.97(7 792.9)	1.18(9 529.9)	
(10,15)	1.49(12 018.3)	1.51(12 190.5)	1.15(9 315.8)	1.24(9 991.4)	1.20(9 678.6)
Gas-phase optimized geometry					
Active space	SA-CASSCF	MS-CASPT2	tPBE	tPBE0	Expt.
(2, 2)	1.94(15 656.5)	1.02(8 261.3)	0.41(3 272.9)	0.79(6 368.8)	
(2, 5)	1.90(15 348.3)	0.98(7 905.2)	0.48(3 906.1)	0.84(6 766.6)	
(2, 10)	1.83(14 776.3)	1.01(8 181.1)	0.52(4 174.7)	0.85(6 825.1)	
(8, 8)	1.85(14 952.6)	1.44(11 604.2)	0.94(7 594.5)	1.17(9 434.0)	
(10, 15)	1.68(13 574.4)	1.43(11 532.2)	1.04(8 393.6)	1.20(9 688.8)	1.20(9 678.6)

1 eV = 8 065.54 cm^{-1}.

Table S10: Calculated triplet-singlet gaps ($\Delta E_{\text{T-S}}$) in eV and cm^{-1} inside the parenthesis, using the unit cell optimized triplet structure of molecule **2**, the experimental structure, and gas-pahse optimized triplet and singlet structures. The energy gaps were obtained with SA-CASSCF, MS-CASPT2, tPBE and tPBE0 methods.

Periodic optimized geometry					
Active Space	SA-CASSCF	MS-CASPT2	tPBE	tPBE0	Expt.
(2, 2)	1.85(14 940.4)	1.20(9 709.1)	0.59(4 770.7)	0.91(7 313.1)	
(2, 5)	1.93(15 013.7)	1.03(9 834.3)	0.48(4 863.5)	0.84(7 401.0)	
(2, 10)	1.86(14 989.6)	1.06(8 554.8)	0.52(4 200.9)	0.86(6 898.1)	
(8, 8)	1.92(15 466.6)	1.43(11 533.3)	0.93(7 536.7)	1.18(9 519.2)	
(10, 15)	1.74(14 069.0)	1.42(11 419.2)	0.94(7 560.4)	1.14(9 187.6)	1.22(9 840.0)
Experimental geometry					
Active Space	SA-CASSCF	MS-CASPT2	tPBE	tPBE0	Expt.
(2,2)	1.86(15 140.7)	1.22(9 904.4)	0.60(4 840.3)	0.92(7 415.4)	
(2,5)	1.94(15 550.7)	1.04(8 276.4)	0.49(3 873.9)	0.86(6 793.1)	
(2,10)	1.87(15 081.8)	1.08(8 673.8)	0.53(4 312.0)	0.87(7 004.4)	
(8,8)	1.89(15 283.5)	1.47(11 871.3)	0.96(7 778.5)	1.20(9 654.7)	
(10,15)	1.64(13 244.8)	1.52(12 279.4)	1.13(9 134.9)	1.26(10 162.4)	1.22(9 840.0)
Gas-phase optimized geometry					
Active space	SA-CASSCF	MS-CASPT2	tPBE	tPBE0	Expt.
(2, 2)	1.94(15 676.7)	1.02(8 216.1)	0.41(3 295.8)	0.79(6 391.1)	
(2, 5)	1.91(15 394.5)	0.98(7 909.3)	0.49(3 923.5)	0.84(6 791.2)	
(2, 10)	1.84(14 820.5)	1.02(8 216.1)	0.52(4 199.9)	0.85(6 855.0)	
(8, 8)	1.86(14 978.7)	1.45(11 681.3)	0.95(7 665.6)	1.18(9 493.9)	
(10, 15)	1.69(13 656.7)	1.44(11 631.1)	1.05(8 471.4)	1.21(9 767.7)	1.22(9 840.0)

1 eV = 8 065.54 cm^{-1}.

Table S11: Calculated triplet-singlet gaps ($\Delta E_{\text{T-S}}$) in eV and cm^{-1} inside the parenthesis, using the unit cell optimized triplet structure of molecule **3**, the experimental structure, and gas-pahse optimized triplet and singlet structures. The energy gaps were obtained with SA-CASSCF, MS-CASPT2, tPBE and tPBE0 methods.

Periodic optimized geometry					
Active Space	SA-CASSCF	MS-CASPT2	tPBE	tPBE0	Expt.
(2, 2)	1.87(15 074.6)	1.21(9 755.7)	0.59(4 791.9)	0.91(7 362.6)	
(2, 5)	1.93(15 539.5)	1.07(8 624.7)	0.47(3 798.5)	0.83(6 733.7)	
(2, 10)	1.86(14 991.9)	1.11(8 963.0)	0.51(4 143.3)	0.85(6 855.4)	
(8, 8)	1.89(15 222.7)	1.45(11 676.8)	0.92(7 406.6)	1.16(9 360.7)	
(10, 15)	1.76(14 168.5)	1.35(10 919.3)	0.93(7 514.6)	1.14(9 178.1)	1.20(9 678.6)
Experimental geometry					
Active Space	SA-CASSCF	MS-CASPT2	tPBE	tPBE0	Expt.
(2,2)	1.88(15 140.7)	1.23(9 904.4)	0.60(4 840.3)	0.92(7 415.4)	
(2,5)	1.94(15 618.6)	1.08(8 728.6)	0.49(3 926.9)	0.85(6 849.8)	
(2,10)	1.87(15 073.7)	1.13(9 132.7)	0.53(4 312.0)	0.86(7 004.4)	
(8,8)	1.90(15 309.9)	1.47(11 839.8)	0.94(7 547.1)	1.18(9 487.8)	
(10,15)	1.56(12 615.7)	1.56(12 613.5)	1.16(9 361.1)	1.26(10 174.8)	1.20(9 678.6)
Gas-phase optimized geometry					
Active space	SA-CASSCF	MS-CASPT2	tPBE	tPBE0	Expt.
(2, 2)	1.93(15 563.6)	0.99(7 973.1)	0.40(3 226.9)	0.78(6 311.0)	
(2, 5)	1.89(15 259.9)	0.96(7 712.9)	0.48(3 868.7)	0.83(6 716.5)	
(2, 10)	1.82(14 681.8)	0.99(7 973.1)	0.51(4 129.5)	0.83(6 767.6)	
(8, 8)	1.84(14 869.9)	1.43(11 507.4)	0.94(7 586.2)	1.17(9 407.2)	
(10, 15)	1.68(13 511.0)	1.42(11 456.1)	1.03(8 333.6)	1.19(9 627.9)	1.20(9 678.6)

1 eV = 8 065.54 cm^{-1}.

5 MS-CASPT2 energy spectra

Calculated energy spectra of complexes **1**, **2**, and **3**, calculated with MS-CASPT2 method. The spectra is calculated for (2,5), (2,10), (8,8) and (10,15) active spaces.

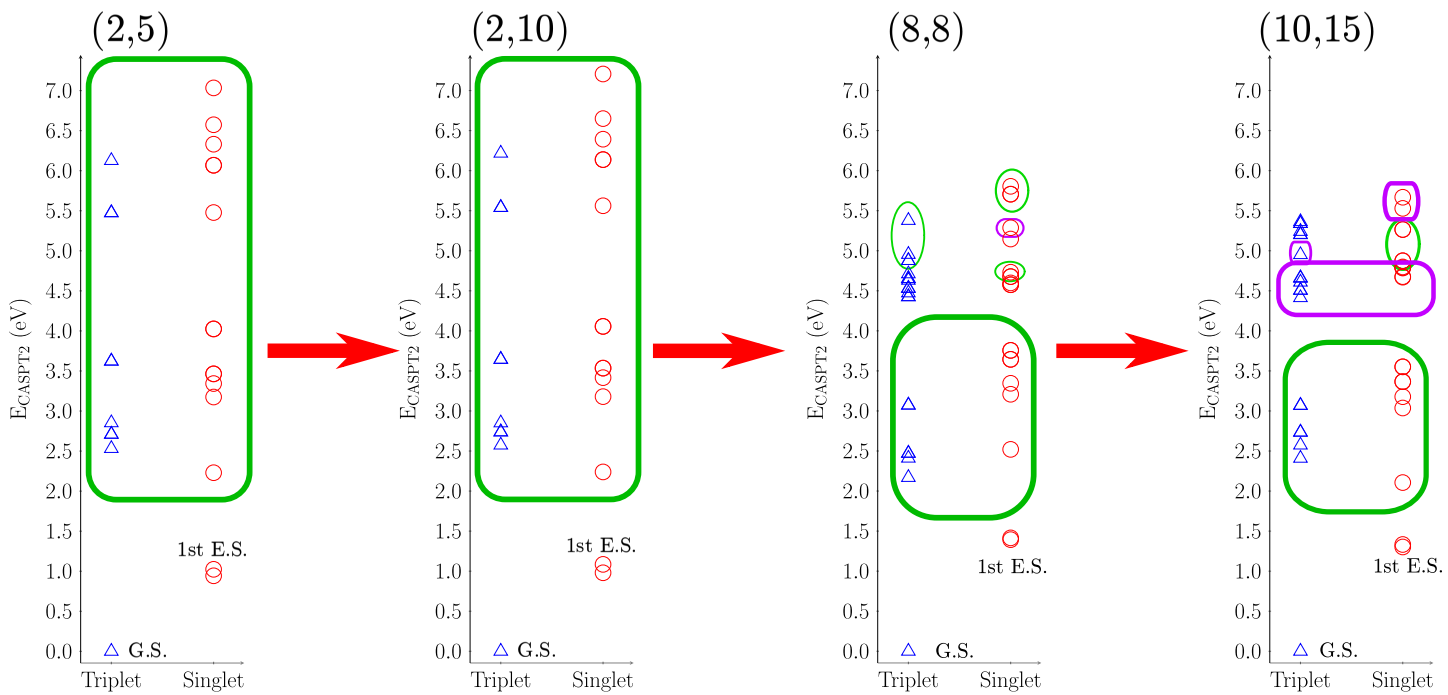

Figure S12: MS-CASPT2 energy plots of the complex **1** periodic optimized geometry. For (2,5) and (2,10) active spaces were computed 10 triplet and 15 singlet states, and 20 lowest-lying triplet and singlet states, each for (8,8), and (10,15) active spaces. The blue triangles correspond to triplet states, and the red circles are for singlet states. In green are highlighted the metal-to-ligand charge transfer states, in purple the ligand-to-metal charge transfer states, and for (8,8) and (10,15), the states without any color box are ligand-to-ligand charge transfer states.

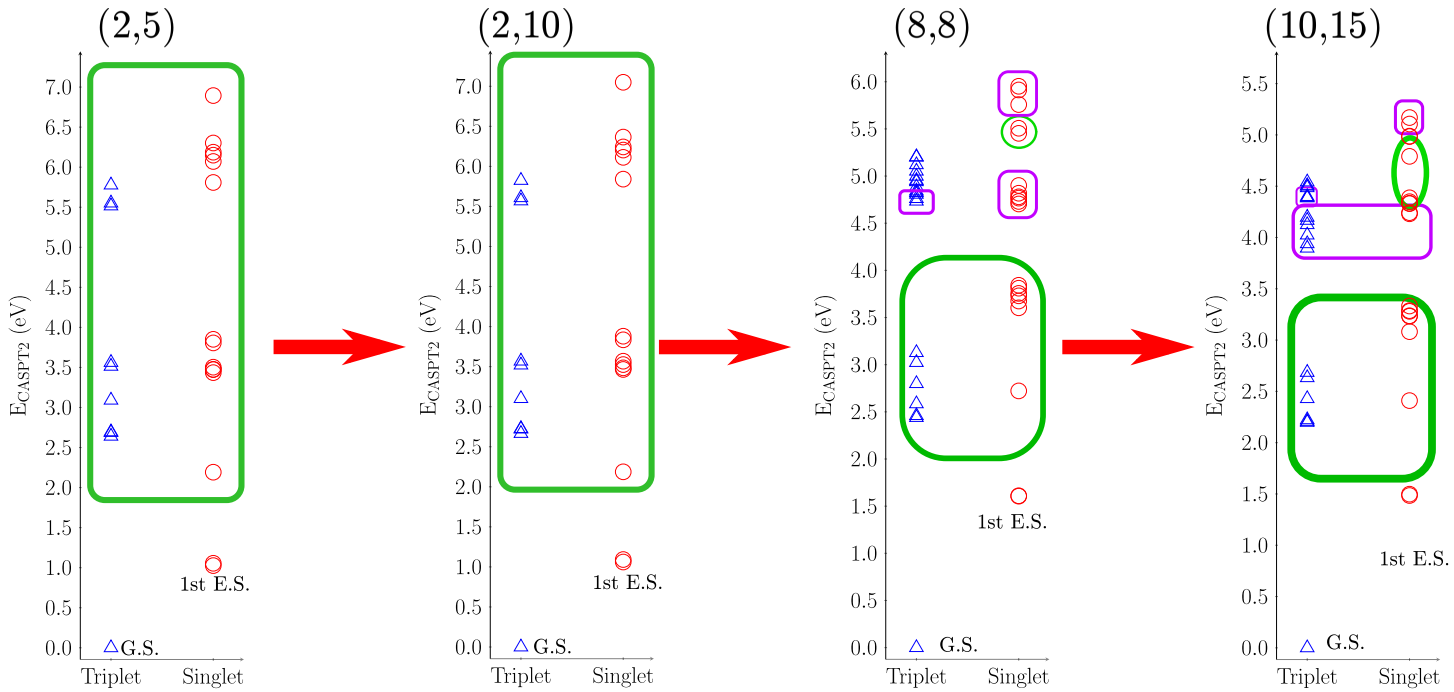

Figure S13: MS-CASPT2 energy plots of the complex **2** periodic optimized geometry. For (2,5) and (2,10) active spaces were computed 10 triplet and 15 singlet states, and 20 lowest-lying triplet and singlet states, each for (8,8), and (10,15) active spaces. The blue triangles correspond to triplet states, and the red circles are for singlet states. In green are highlighted the metal-to-ligand charge transfer states, in purple the ligand-to-metal charge transfer states, and for (8,8) and (10,15), the states without any color box are ligand-topligand charge transfer states.

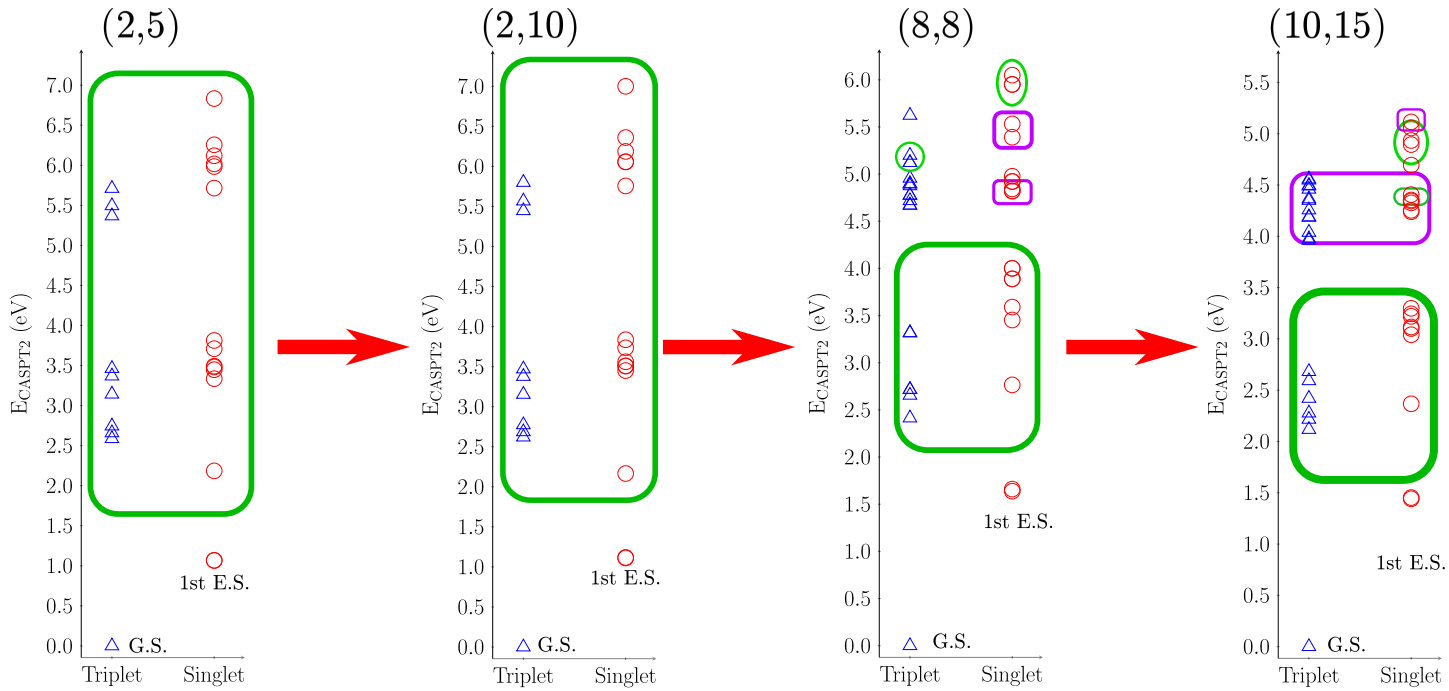

Figure S14: MS-CASPT2 energy plots of the complex **3** periodic optimized geometry. For (2,5) and (2,10) active spaces were computed 10 triplet and 15 singlet states, and 20 lowest-lying triplet and singlet states, each for (8,8), and (10,15) active spaces. The blue triangles correspond to triplet states, and the red circles are fpr singlet states. In green are highlighted the metal-to-ligand charge transfer states, in purple the ligand-to-metal charge transfer states, and for (8,8) and (10,15), the states without any color box are ligand-to-ligand charge transfer states.

6 HMC-PDFT energy spectra

Calculated energy spectra of complexes **1**, **2**, and **3**, calculated with HMC-PDFT(tPBE0) method. The spectra is calculated for (2,5), (2,10), (8,8) and (10,15) active spaces.

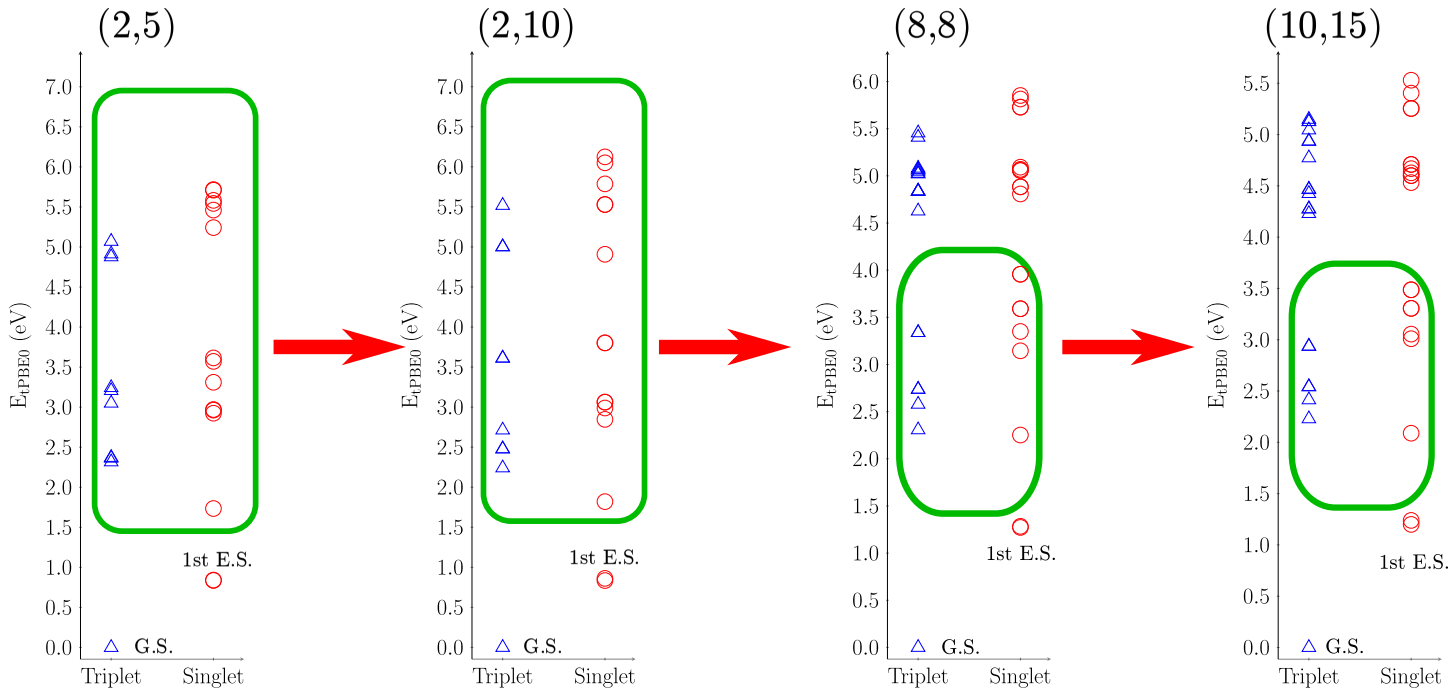

Figure S15: HMC-PDFT(tPBE0) energy plots of the complex **1** periodic optimized geometry. For (2,5) and (2,10) active spaces were computed 10 triplet and 15 singlet states, and 20 lowest-lying triplet and singlet states, each for (8,8), and (10,15) active spaces. The blue triangles correspond to triplet states, and the red circles are for singlet states. In green are highlighted the metal-to-ligand charge transfer states.

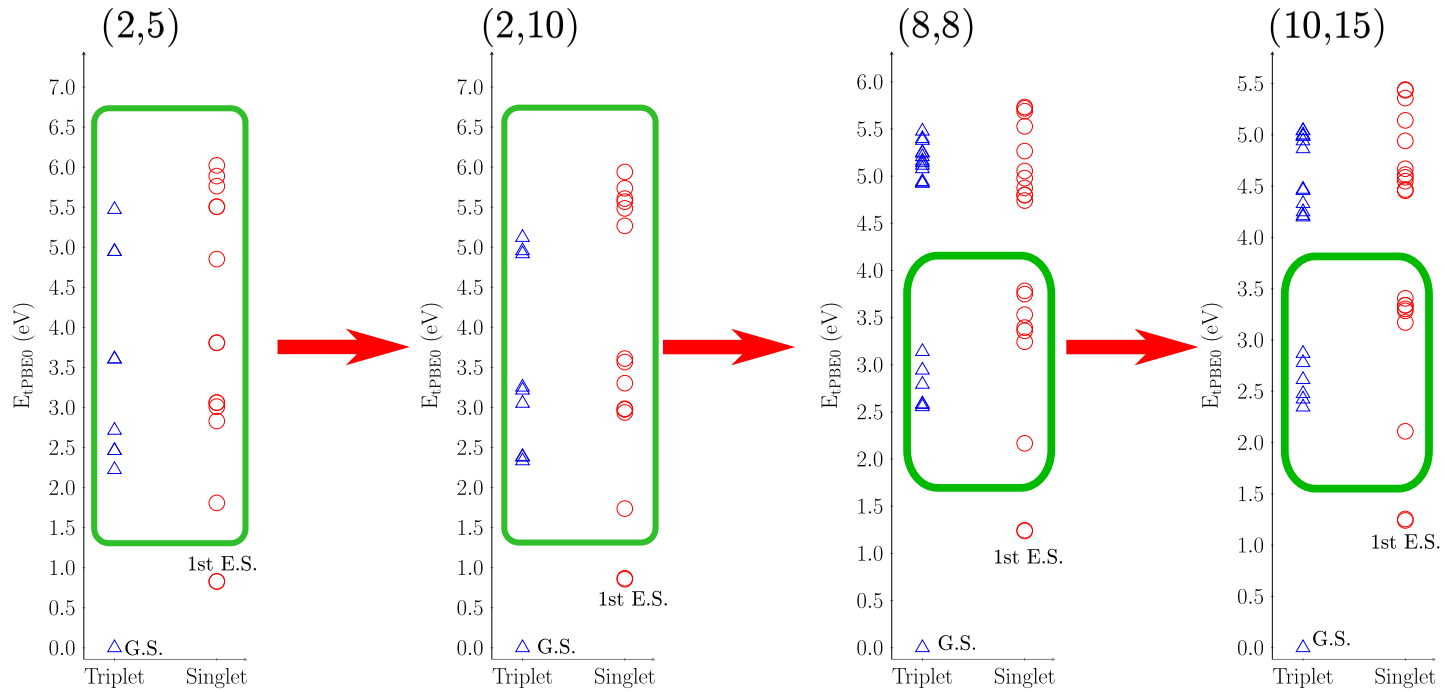

Figure S16: HMC-PDFT(tPBE0) energy plots of the complex **2** periodic optimized geometry. For (2,5) and (2,10) active spaces were computed 10 triplet and 15 singlet states, and 20 lowest-lying triplet and singlet states, each for (8,8), and (10,15) active spaces. The blue triangles correspond to triplet states, and the red circles are for singlet states. In green are highlighted the metal-to-ligand charge transfer states.

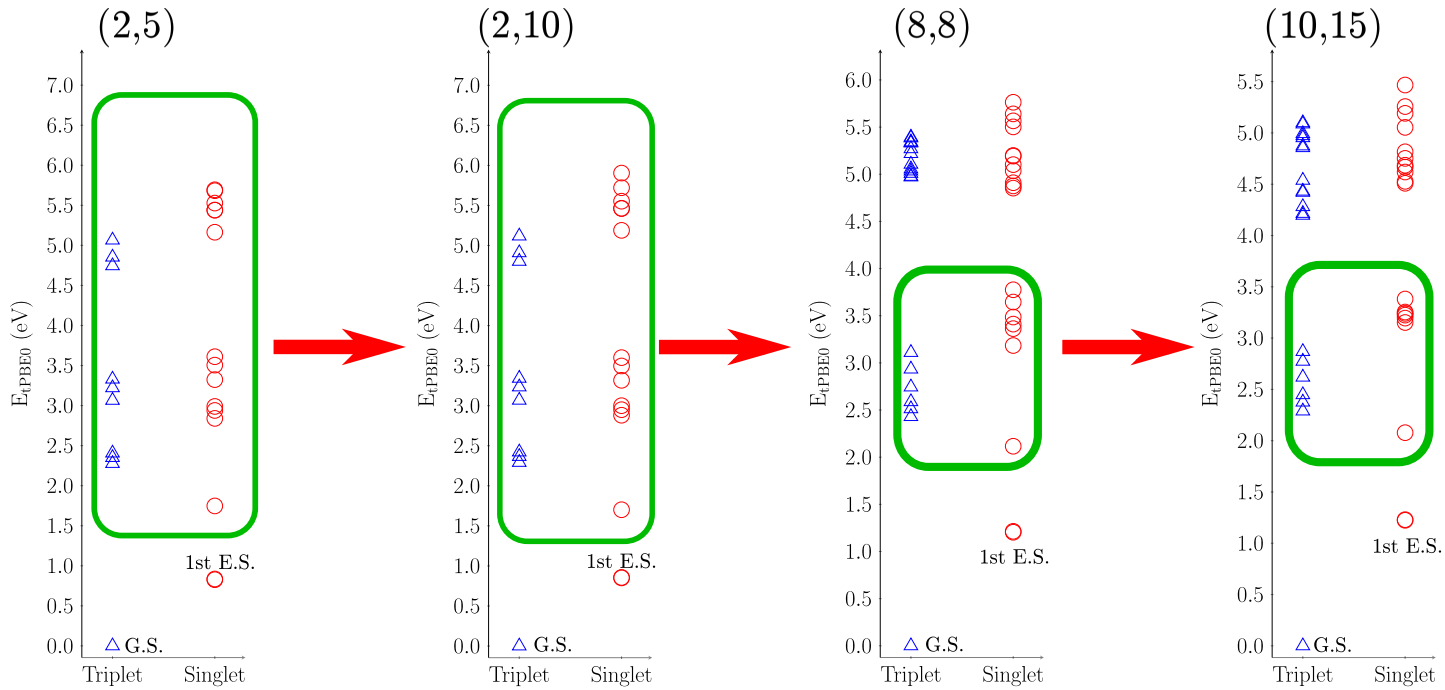

Figure S17: HMC-PDFT(tPBE0) energy plots of the complex **3** periodic optimized geometry. For (2,5) and (2,10) active spaces were computed 10 triplet and 15 singlet states, and 20 lowest-lying triplet and singlet states, each for (8,8), and (10,15) active spaces. The blue triangles correspond to triplet states, and the red circles are for singlet states. In green are highlighted the metal-to-ligand charge transfer states.

7 Zero-field splitting parameters

For complex **1**, the MS-CASPT2 calculation required almost 16 hours to compute the energy of the seven lowest-lying triplet states with (10,15) active space; in comparison the HMC-PDFT calculation required only 1.5 hours—this is a tenfold reduction in compute time as compared to MS-CASPT2.

Table S12: ZFS parameters calculated with the (2,5) active space, using different numbers of triplets and singlets at the periodic optimized geometry of complex **1**. The parameters were computed with SA-CASSCF, MS-CASPT2, MS-PDFT(tPBE), and HMS-PDFT(tPBE0). The values are reported in GHz, and cm^{-1} inside the parenthesis.

	7T-9S		10T-15S		Experiment	
Method	$\|D\|$	$\|E\|$	$\|D\|$	$\|E\|$	$\|D\|$	$\|E\|$
SA-CASSCF	11.27(0.376)	0.00(0.000)	11.33(0.378)	0.00(0.000)	3.53(0.118)	0.00(0.000)
MS-CASPT2	3.53(0.118)	0.01(0.000)	3.66(0.122)	0.01(0.000)		
tPBE	0.98(0.033)	0.00(0.000)	1.12(0.037)	0.00(0.000)		
tPBE0	3.59(0.120)	0.00(0.000)	3.71(0.124)	0.00(0.000)		

1 GHz = 29.9793 cm^{-1}.

Table S13: ZFS parameters calculated with the (2,10) active space, using different numbers of triplets and singlets at the periodic optimized geometry of complex **1**. The parameters were computed with SA-CASSCF, MS-CASPT2, MS-PDFT(tPBE), and HMS-PDFT(tPBE0). The values are reported in GHz, and cm^{-1} inside the parenthesis.

	7T-9S		10T-15S		Experiment	
Method	$\|D\|$	$\|E\|$	$\|D\|$	$\|E\|$	$\|D\|$	$\|E\|$
SA-CASSCF	10.41(0.347)	0.00(0.000)	10.39(0.347)	0.00(0.000)	3.53(0.118)	0.00(0.000)
MS-CASPT2	2.73(0.091)	0.01(0.000)	2.80(0.093)	0.00(0.000)		
tPBE	2.59(0.086)	0.00(0.000)	0.92(0.031)	0.00(0.000)		
tPBE0	4.72(0.157)	0.00(0.000)	3.24(0.108)	0.00(0.000)		

1 GHz = 29.9793 cm^{-1}.

Table S14: ZFS parameters calculated with the (8,8) active space, using different numbers of triplets and singlets at the periodic optimized geometry of complex **1**. The parameters were computed with SA-CASSCF, MS-PDFT(tPBE), and HMS-PDFT(tPBE0). The values are reported in GHz, and cm^{-1} inside the parenthesis.

	7T-9S		18T-16S		Experiment	
Method	$\|D\|$	$\|E\|$	$\|D\|$	$\|E\|$	$\|D\|$	$\|E\|$
SA-CASSCF	6.27(0.209)	0.00(0.000)	5.98(0.199)	0.00(0.000)	3.53(0.118)	0.00(0.000)
MS-CASPT2	3.33(0.111)	0.00(0.000)	2.92(0.097)	0.00(0.000)		
tPBE	3.05(0.102)	0.00(0.000)	2.16(0.072)	0.00(0.000)		
tPBE0	4.26(0.142)	0.00(0.000)	3.49(0.116)	0.00(0.000)		

1 GHz = 29.9793 cm^{-1}.

Table S15: ZFS parameters calculated with the (10,15) active space, using different numbers of triplets and singlets at theperiodic optimized geometry of complex **1**. The parameters were computed with SA-CASSCF, MS-CASPT2, MS-PDFT(tPBE), and HMS-PDFT(tPBE0). The values are reported in GHz, and cm^{-1} inside the parenthesis.

	7T-9S		13T-16S		16T-15S	
Method	$\|D\|$	$\|E\|$	$\|D\|$	$\|E\|$	$\|D\|$	$\|E\|$
SA-CASSCF	4.48(0.149)	0.00(0.000)	4.07(0.136)	0.00(0.000)	2.65(0.088)	0.00(0.000)
MS-CASPT2	3.65(0.122)	0.00(0.000)	5.14(0.171)	0.00(0.000)	1.27(0.042)	0.00(0.000)
tPBE	0.73(0.024)	0.00(0.000)	1.21(0.040)	0.00(0.000)	0.32(0.011)	0.00(0.000)
tPBE0	2.07(0.069)	0.00(0.000)	2.28(0.076)	0.00(0.000)	0.78(0.026)	0.00(0.000)

1 GHz = 29.9793 cm^{-1}.

Table S16: ZFS parameters calculated with the (2,5) active space, using different numbers of triplets and singlets at the periodic optimized geometry of complex **2**. The parameters were computed with SA-CASSCF, MS-CASPT2, MS-PDFT(tPBE), and HMS-PDFT(tPBE0). The values are reported in GHz, and cm^{-1} inside the parenthesis.

	7T-9S		10T-15S		Experiment	
Method	$\|D\|$	$\|E\|$	$\|D\|$	$\|E\|$	$\|D\|$	$\|E\|$
SA-CASSCF	1.22(0.041)	0.33(0.011)	1.00(0.033)	0.69(0.023)	1.92(0.064)	0.53(0.018)
MS-CASPT2	1.34(0.045)	0.32(0.011)	0.80(0.027)	0.07(0.002)		
tPBE	0.34(0.011)	0.28(0.009)	1.30(0.043)	0.27(0.009)		
tPBE0	0.59(0.020)	0.23(0.008)	0.85(0.028)	0.42(0.014)		

1 GHz = 29.9793 cm^{-1}.

Table S17: ZFS parameters calculated with the (2,10) active space, using different numbers of triplets and singlets at the periodic optimized geometry of complex **2** . The parameters were computed with SA-CASSCF, CASPT2, MS-PDFT(tPBE), and HMS-PDFT(tPBE0). The values are reported in GHz, and cm^{-1} inside the parenthesis.

	7T-9S		10T-15S		Experiment	
Method	$\|D\|$	$\|E\|$	$\|D\|$	$\|E\|$	$\|D\|$	$\|E\|$
SA-CASSCF	1.24(0.041)	0.19(0.006)	0.97(0.032)	0.53(0.018)	1.92(0.064)	0.53(0.018)
MS-CASPT2	1.16(0.039)	0.20(0.007)	0.72(0.024)	0.10(0.003)		
tPBE	0.31(0.010)	0.25(0.008)	0.98(0.033)	0.26(0.009)		
tPBE0	0.61(0.020)	0.17(0.006)	0.68(0.023)	0.39(0.013)		

1 GHz = 29.9793 cm^{-1}.

Table S18: ZFS parameters calculated with the (8,8) active space, using different numbers of triplets and singlets at the periodic optimized geometry of complex **2**. The parameters were computed with SA-CASSCF, MS-CASPT2, MS-PDFT(tPBE), and HMS-PDFT(tPBE0). The values are reported in GHz, and cm^{-1} inside the parenthesis.

	7T-9S		17T-16S		Experiment	
Method	$\|D\|$	$\|E\|$	$\|D\|$	$\|E\|$	$\|D\|$	$\|E\|$
SA-CASSCF	6.27(0.209)	0.31(0.010)	5.98(0.199)	0.45(0.015)	1.92(0.064)	0.53(0.018)
MS-CASPT2	3.33(0.111)	0.25(0.008)	2.92(0.097)	0.31(0.010)		
tPBE	3.05(0.102)	0.10(0.003)	2.16(0.072)	0.02(0.001)		
tPBE0	4.26(0.142)	0.04(0.001)	3.49(0.116)	0.12(0.004)		

1 GHz = 29.9793 cm^{-1}.

Table S19: ZFS parameters calculated with the (10,15) active space, using different numbers of triplets and singlets at the periodic optimized geometry of complex **2**. The parameters were computed with SA-CASSCF, MS-CASPT2, MS-PDFT(tPBE), and HMS-PDFT(tPBE0). The values are reported in GHz, and cm^{-1} inside the parenthesis.

	7T-9S		13T-16S		Experiment	
Method	$\|D\|$	$\|E\|$	$\|D\|$	$\|E\|$	$\|D\|$	$\|E\|$
SA-CASSCF	1.14(0.038)	0.22(0.007)	2.00(0.067)	0.31(0.010)	1.92(0.064)	0.53(0.018)
MS-CASPT2	1.14(0.038)	0.36(0.012)	2.90(0.097)	0.42(0.014)		
tPBE	1.85(0.062)	0.22(0.007)	0.61(0.020)	0.16(0.005)		
tPBE0	0.81(0.027)	0.19(0.006)	0.82(0.027)	0.19(0.006)		

1 GHz = 29.9793 cm^{-1}.

Table S20: ZFS parameters calculated with the (2,5) active space, using different nnumbers of triplets and singlets at the periodic optimized geometry of complex **3**. The parameters were computed with SA-CASSCF, MS-CASPT2, MS-PDFT(tPBE), and HMS-PDFT(tPBE0). The values are reported in GHz, and cm^{-1} inside the parenthesis.

	7T-9S		10T-15S		Experiment	
Method	$\|D\|$	$\|E\|$	$\|D\|$	$\|E\|$	$\|D\|$	$\|E\|$
SA-CASSCF	4.45(0.148)	1.15(0.038)	4.52(0.151)	1.20(0.040)	4.19(0.139)	0.48(0.016)
MS-CASPT2	2.72(0.091)	0.82(0.027)	1.65(0.055)	0.21(0.007)		
tPBE	1.30(0.043)	0.30(0.010)	3.55(0.118)	0.38(0.013)		
tPBE0	2.07(0.069)	0.62(0.021)	1.22(0.041)	0.31(0.010)		

1 GHz = 29.9793 cm^{-1}.

Table S21: ZFS parameters calculated with the (2,10) active space, using different numbers of triplets and singlets at the periodic optimized geometry of complex **3**. The parameters were computed with SA-CASSCF, MS-CASPT2, MS-PDFT(tPBE), and HMS-PDFT(tPBE0).The values are reported in GHz, and cm^{-1} inside the parenthesis.

	7T-9S		10T-15S		Experiment	
Method	$\|D\|$	$\|E\|$	$\|D\|$	$\|E\|$	$\|D\|$	$\|E\|$
SA-CASSCF	4.25(0.142)	1.06(0.035)	4.17(0.139)	1.09(0.036)	4.19(0.139)	0.48(0.016)
MS-CASPT2	2.43(0.081)	0.76(0.025)	2.04(0.068)	0.55(0.018)		
tPBE	1.36(0.045)	0.41(0.014)	0.86(0.029)	0.04(0.001)		
tPBE0	2.11(0.070)	0.58(0.019)	1.52(0.051)	0.49(0.016)		

1 GHz = 29.9793 cm^{-1}.

Table S22: ZFS parameters calculated with the (8,8) active space, using different numbers of triplets and singlets at the periodic optimized geometry of complex **3**. The parameters were computed with SA-CASSCF, MS-CASPT2, MS-PDFT(tPBE), and HMS-PDFT(tPBE0). The values are reported in GHz, and cm^{-1} inside the parenthesis.

	7T-9S		15T-16S		Experiment	
Method	$\|D\|$	$\|E\|$	$\|D\|$	$\|E\|$	$\|D\|$	$\|E\|$
SA-CASSCF	2.95(0.098)	0.46(0.015)	3.42(0.114)	0.66(0.022)	4.19(0.139)	0.48(0.016)
MS-CASPT2	2.69(0.090)	0.76(0.025)	2.50(0.083)	1.90(0.063)		
tPBE	1.76(0.059)	0.31(0.010)	3.65(0.122)	0.92(0.031)		
tPBE0	0.93(0.031)	0.20(0.007)	2.89(0.096)	0.94(0.031)		

1 GHz = 29.9793 cm^{-1}.

Table S23: ZFS parameters calculated with the (10,15) active space, using different numbers of triplets and singlets at the periodic optimized geometry of complex **3**. The parameters were computed with SA-CASSCF, MS-CASPT2, MS-PDFT(tPBE), and HMS-PDFT(tPBE0). The values are reported in GHz, and cm^{-1} inside the parenthesis.

	7T-9S		13T-16S		Experiment	
Method	$\|D\|$	$\|E\|$	$\|D\|$	$\|E\|$	$\|D\|$	$\|E\|$
SA-CASSCF	2.43(0.081)	0.28(0.009)	3.10(0.103)	0.26(0.009)	4.19(0.139)	0.48(0.016)
MS-CASPT2	2.14(0.071)	0.28(0.009)	3.39(0.113)	0.37(0.012)		
tPBE	0.72(0.024)	0.50(0.017)	3.65(0.122)	0.01(0.000)		
tPBE0	1.08(0.036)	0.22(0.007)	3.47(0.116)	0.09(0.003)		

1 GHz = 29.9793 cm^{-1}.

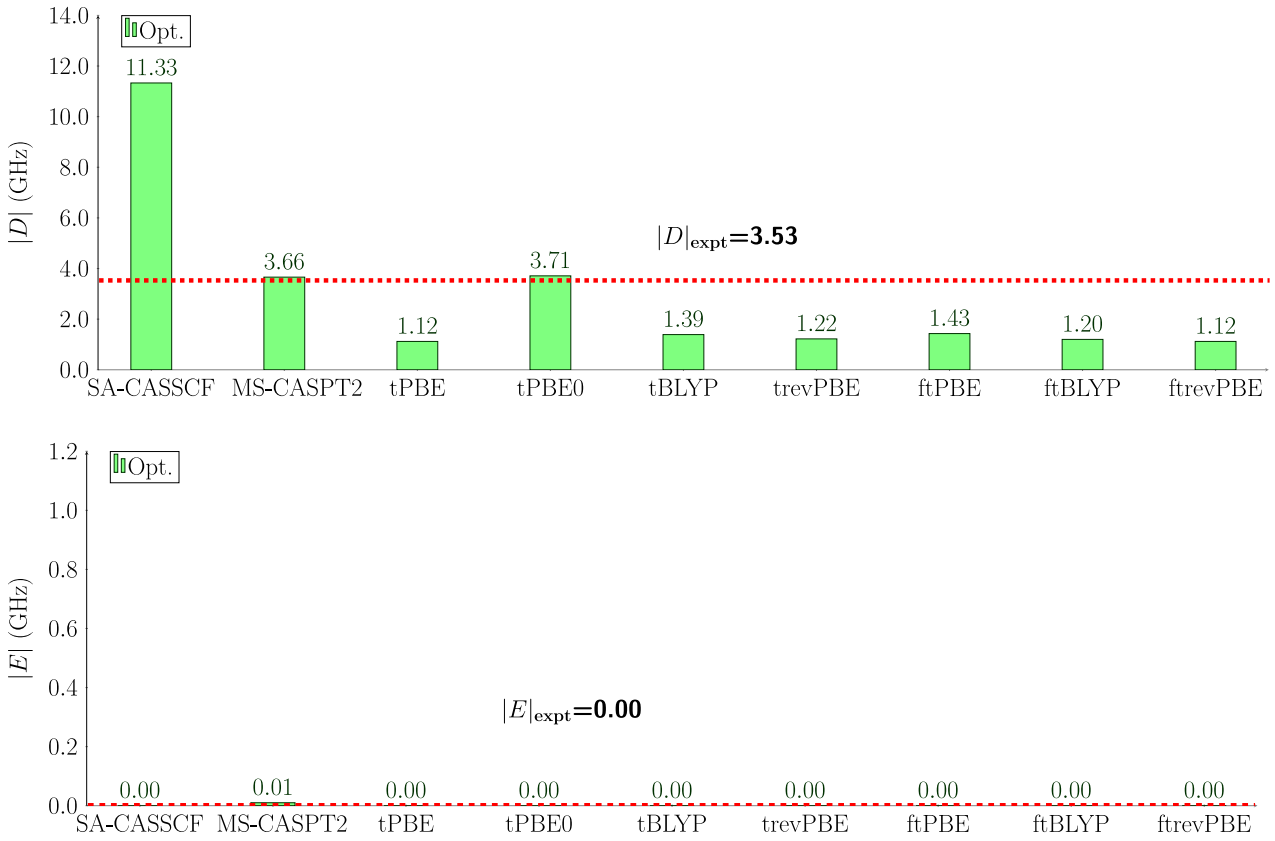

Figure S18: Computed ZFS parameters $|D|$ and $|E|$ of complex **1** with SA-CASSCF, MS-CASPT2, the translated on-top functionals tPBE, tBLYP, and trevPBE, the fully translated on-top functionals ftPBE, ftBLYP, and ftrevPBE, and the hybrid tPBE0 method. The active space is (2,5), and it was used the lowest-lying 10 triplets and 15 singlets states. The horizontal red line represents the experimental values reported in reference.[S25]

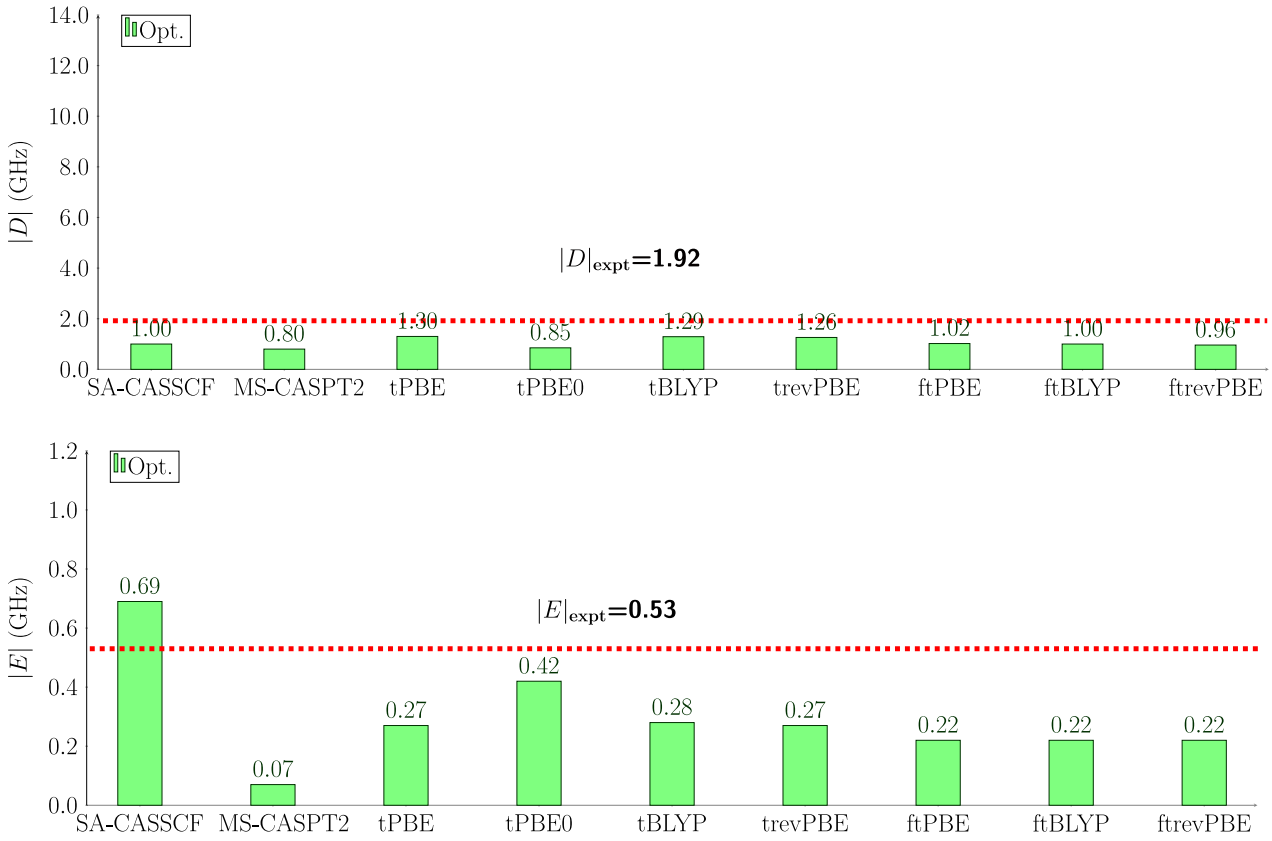

Figure S19: Computed ZFS parameters $|D|$ and $|E|$ of complex **2** with SA-CASSCF, MS-CASPT2, the translated on-top functionals tPBE, tBLYP, and trevPBE, the fully translated on-top functionals ftPBE, ftBLYP, and ftrevPBE, and the hybrid tPBE0 method. The active space is (2,5), and it was used the lowest-lying 10 triplets and 15 singlets states. The horizontal red line represents the experimental values reported in reference.[S25]

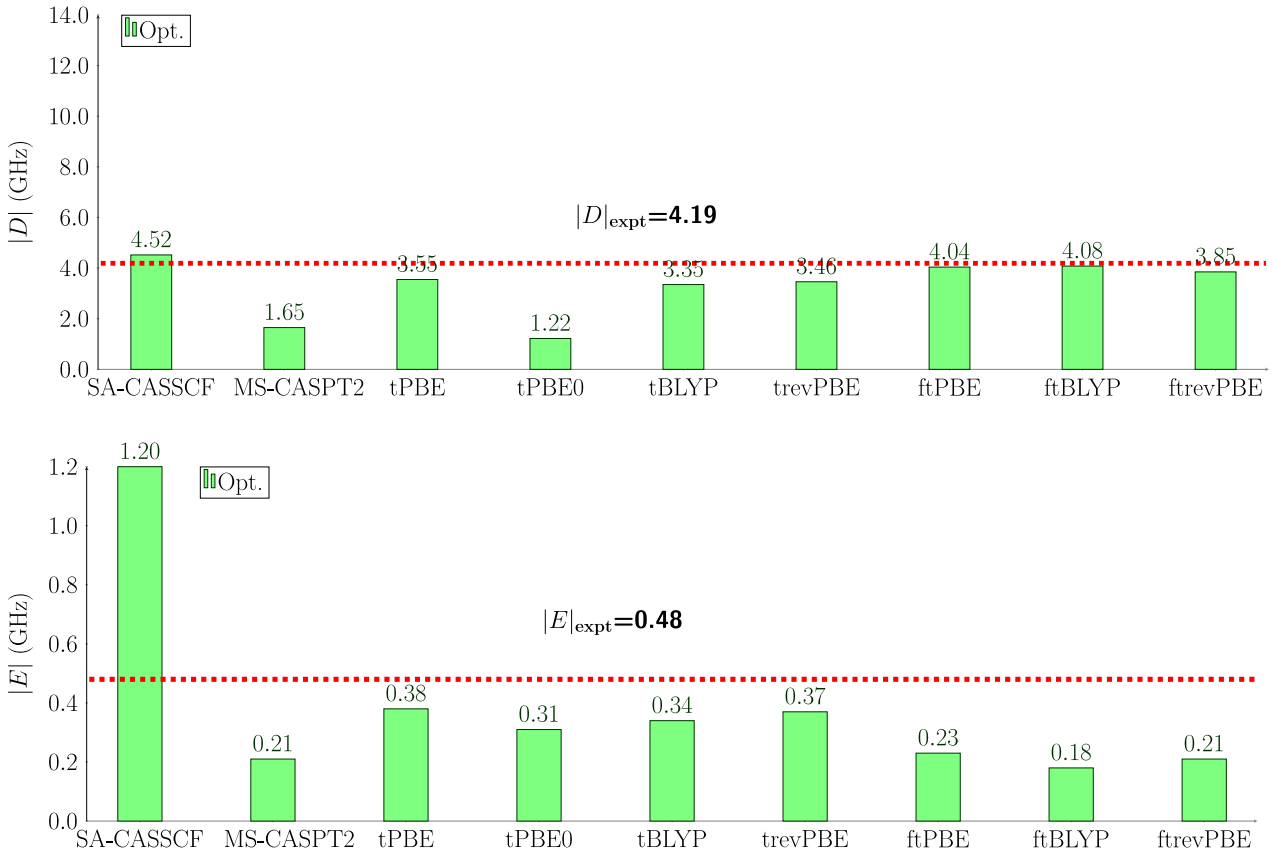

Figure S20: Computed ZFS parameters $|D|$ and $|E|$ of complex **3** with SA-CASSCF, MS-CASPT2, the translated on-top functionals tPBE, tBLYP, and trevPBE, the fully translated on-top functionals ftPBE, ftBLYP, and ftrevPBE, and the hybrid tPBE0 method. The active space is (2,5), and it was used the lowest-lying 10 triplets and 15 singlets states. The horizontal red line represents the experimental values reported in reference.[S25]

8 Trends using different active spaces

8.1 Structures optimized with periodic calculations

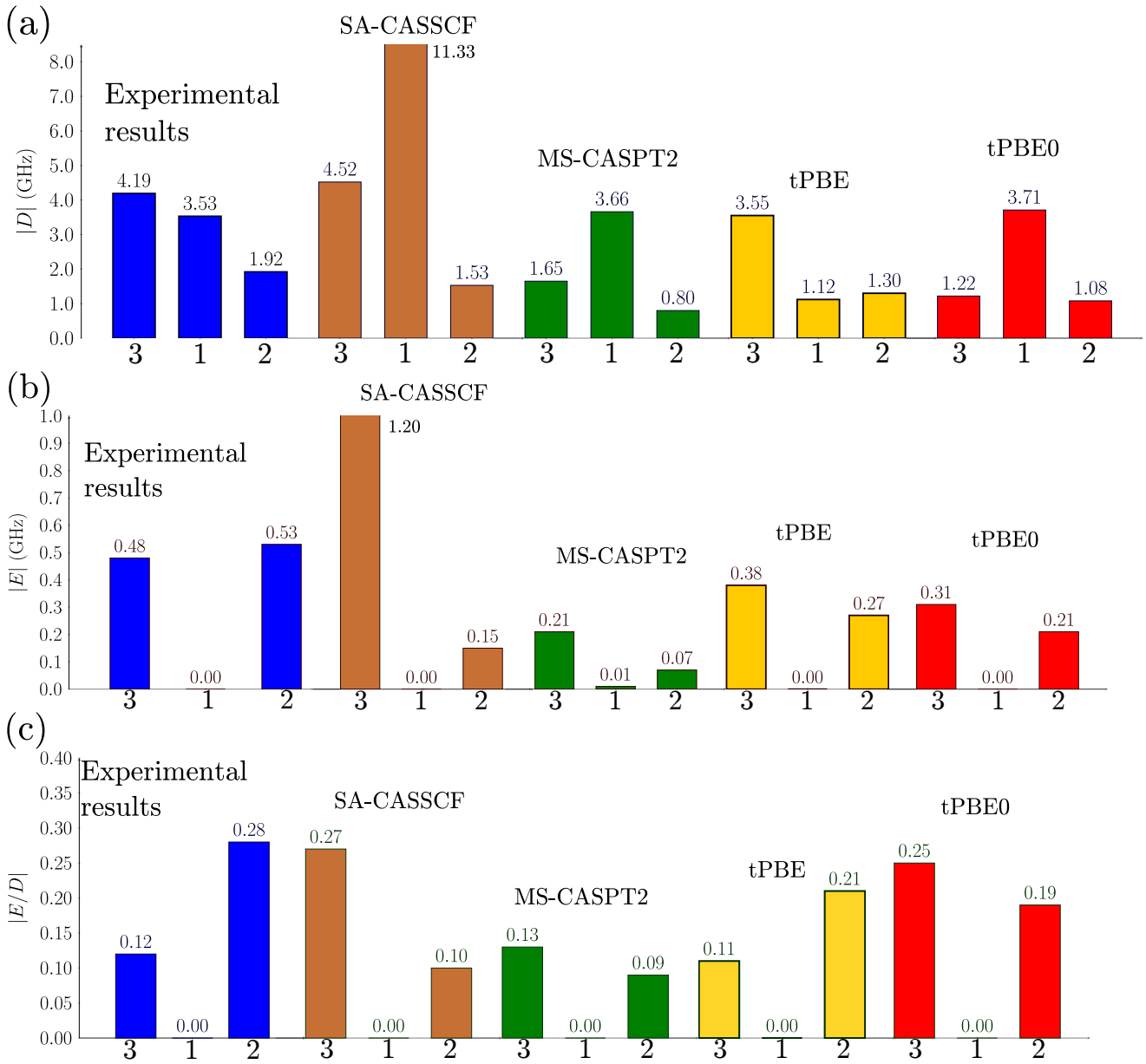

Figure S21: Trends of experimental and calculated values using the (2,5) active space for (a) the axial ZFS parameter $|D|$, (b) the rhombic ZFS parameter $|E|$, and (c) the ratio $|E/D|$. The blue bars correspond to the experimental measurements, and the other bars are for the following electronic structure methods: SA-CASSCF (brown), MS-CASPT2 (green), MS-PDFT(tPBE) (yellow), and HMS-PDFT(tPBE0) (red).

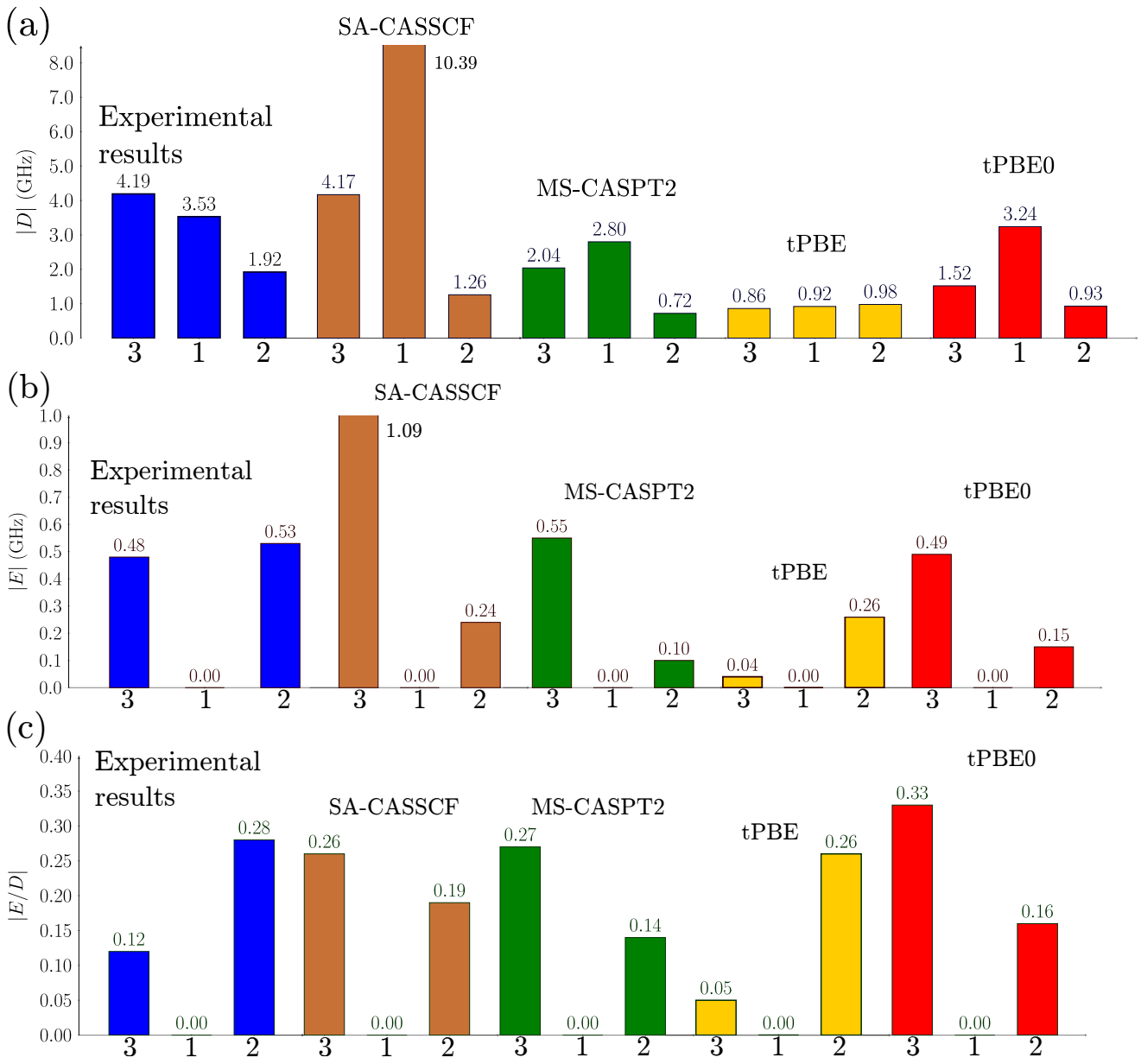

Figure S22: Trends of experimental and calculated values using the (2,10) active space for (a) the axial ZFS parameter $|D|$, (b) the rhombic ZFS parameter $|E|$, and (c) the ratio $|E/D|$. The blue bars correspond to the experimental measurements, and the other bars are for the following electronic structure methods: SA-CASSCF (brown), MS-CASPT2 (green), MS-PDFT(tPBE) (yellow), and HMS-PDFT(tPBE0) (red).

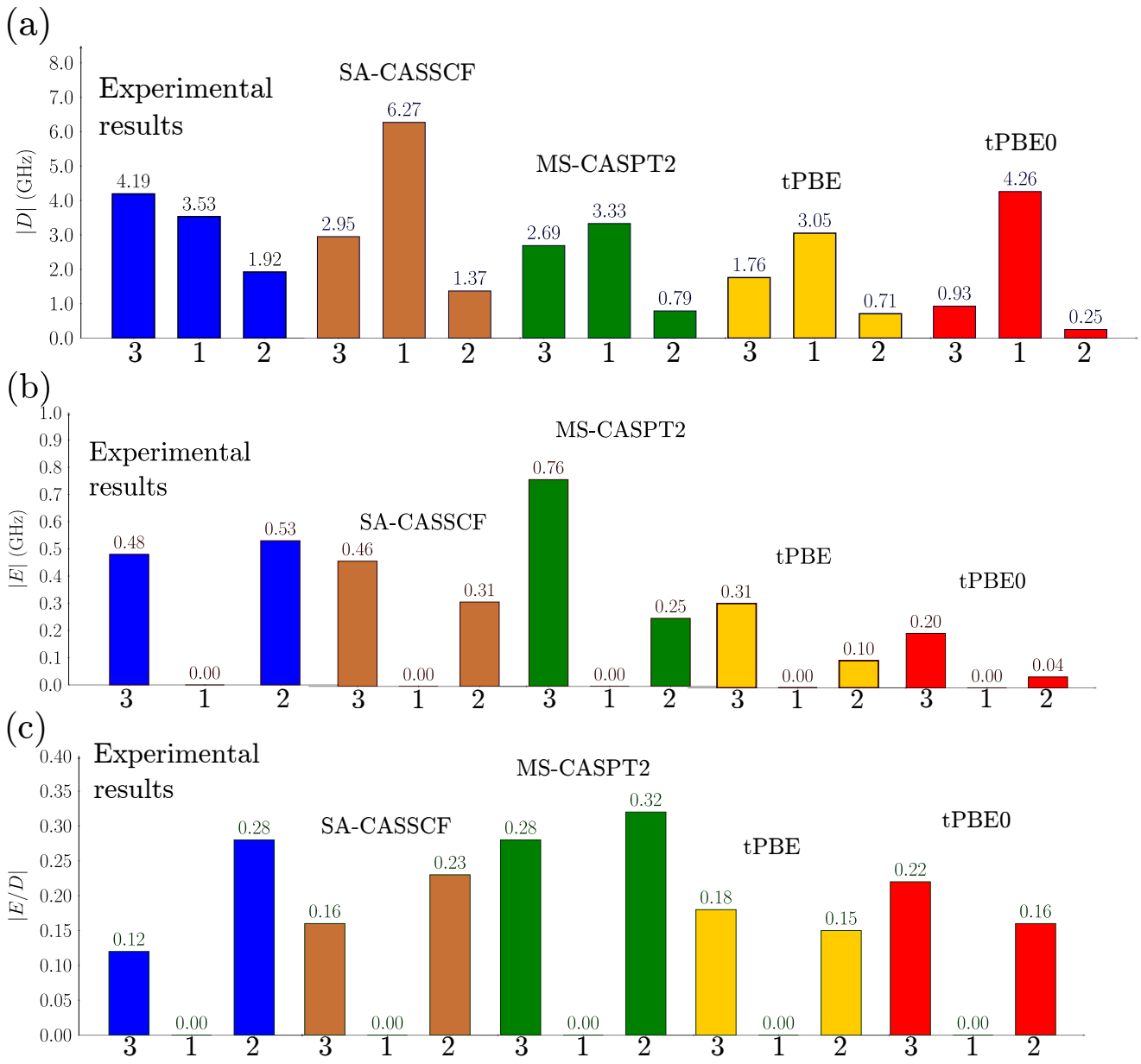

Figure S23: Trends of experimental and calculated values using the (8,8) active space for (a) the axial ZFS parameter $|D|$, (b) the rhombic ZFS parameter $|E|$, and (c) the ratio $|E/D|$. The blue bars correspond to the experimental measurements, and the other bars are for the following electronic structure methods: SA-CASSCF (brown), MS-CASPT2 (green), MS-PDFT(tPBE) (yellow), and HMS-PDFT(tPBE0) (red).

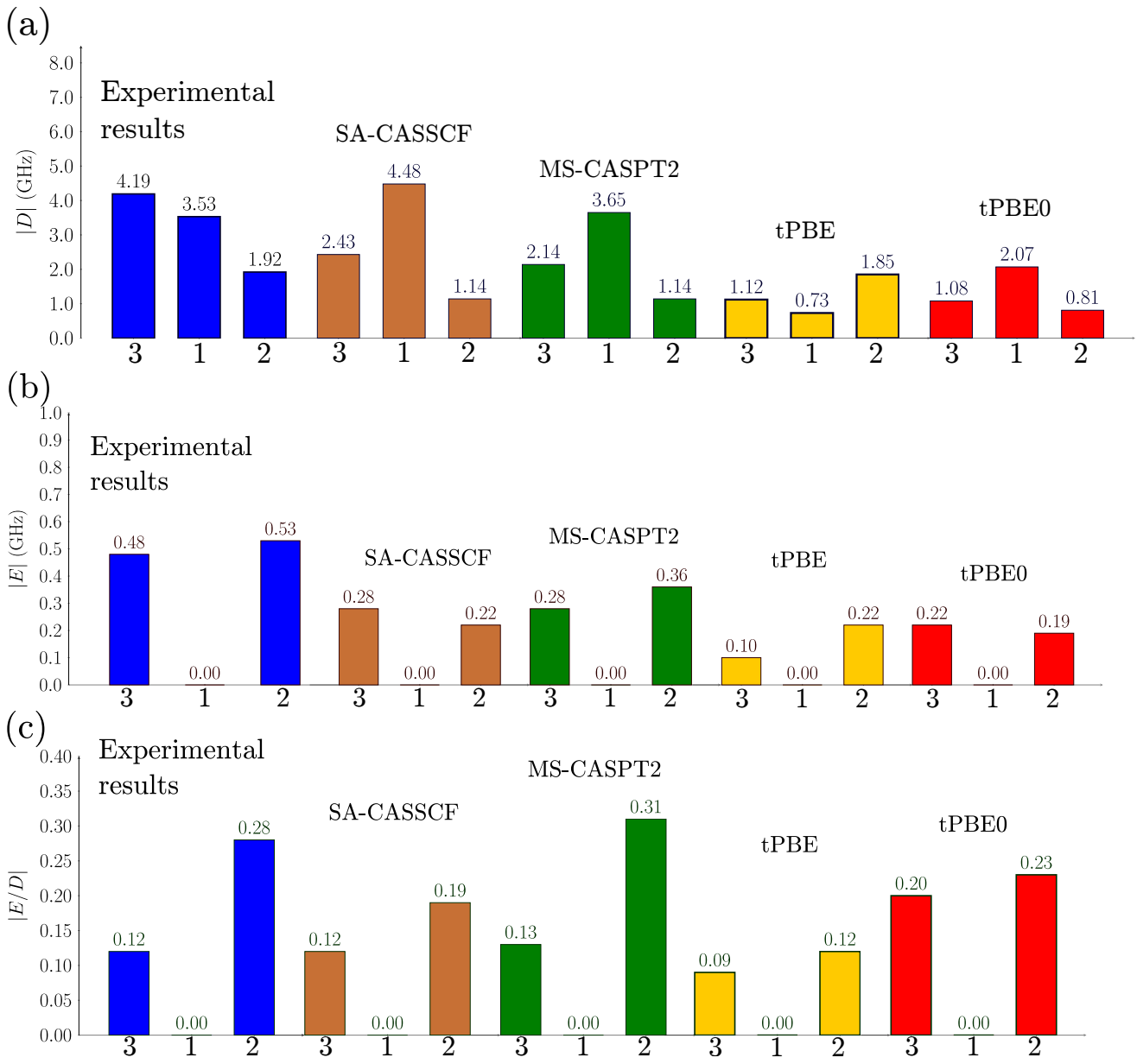

Figure S24: Trends of experimental and calculated values using the (10,15) active space for (a) the axial ZFS parameter $|D|$, (b) the rhombic ZFS parameter $|E|$, and (c) the ratio $|E/D|$. The blue bars correspond to the experimental measurements, and the other bars are for the following electronic structure methods: SA-CASSCF (brown), MS-CASPT2 (green), MS-PDFT(tPBE) (yellow), and HMS-PDFT(tPBE0) (red).

8.2 Structures optimized in gas-phase

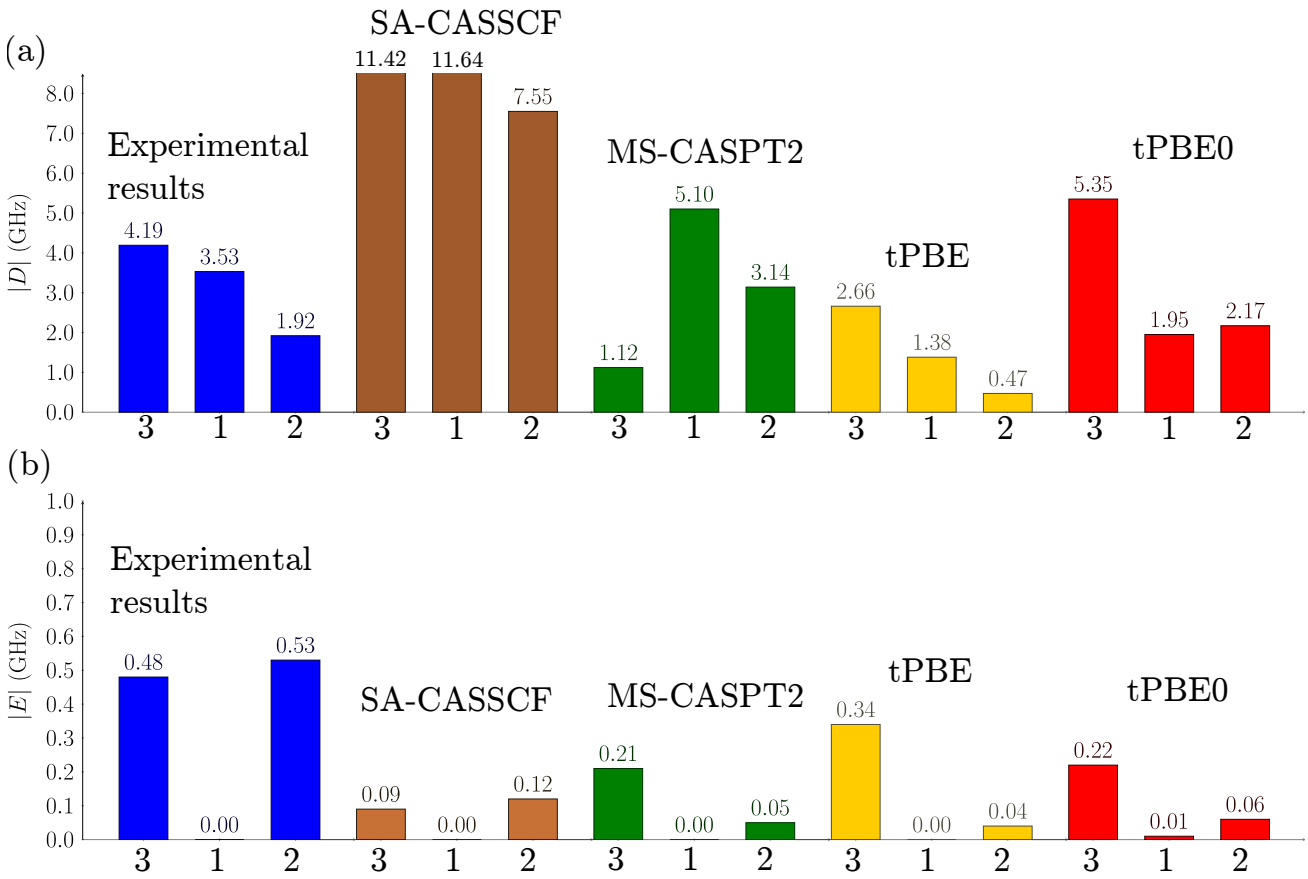

Figure S25: Trends of experimental and calculated values using the (2,5) active space for (a) the axial ZFS parameter $|D|$, and (b) the rhombic ZFS parameter $|E|$. The blue bars correspond to the experimental measurements, and the other bars are for the following electronic structure methods: SA-CASSCF (brown), MS-CASPT2 (green), MS-PDFT(tPBE) (yellow), and HMS-PDFT(tPBE0) (red).

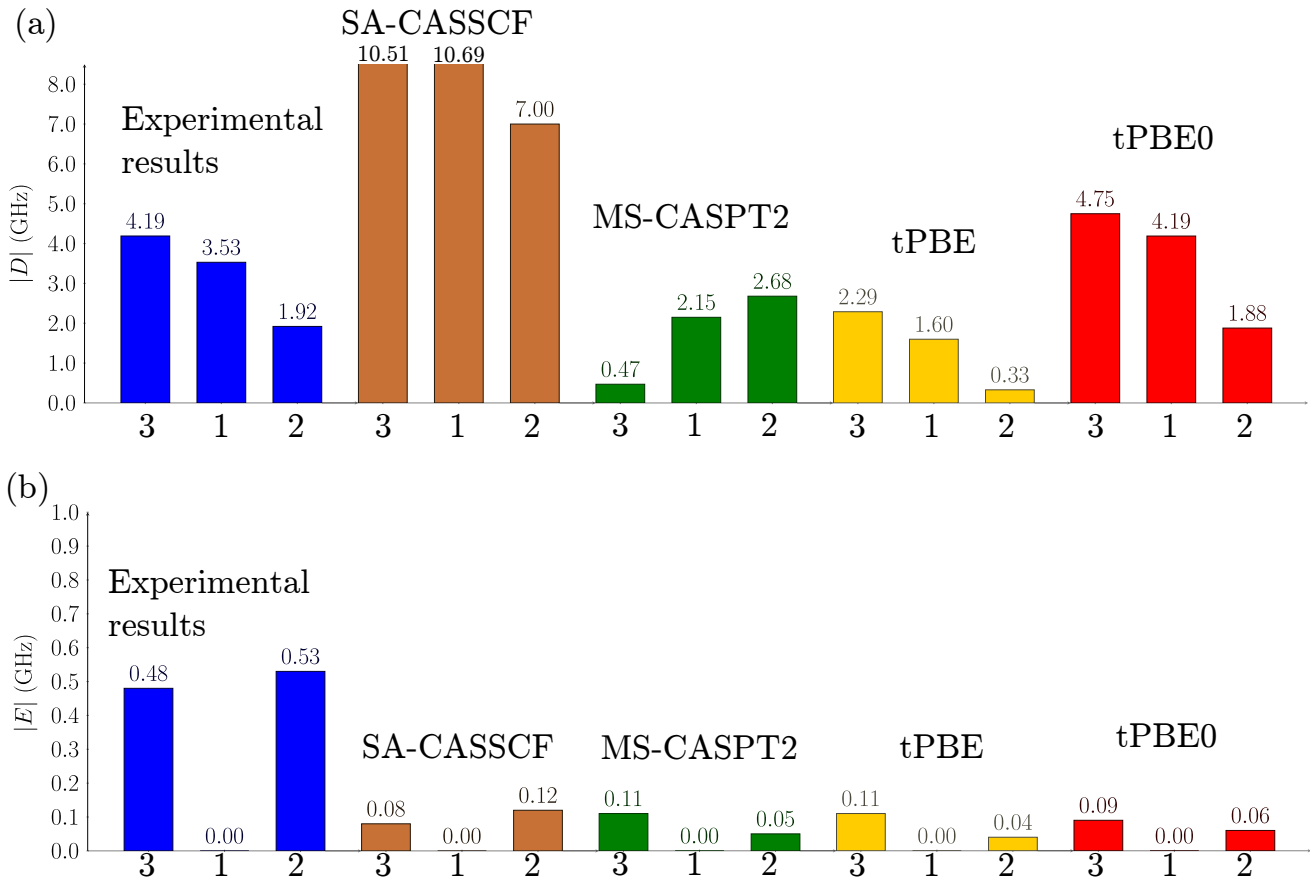

Figure S26: Trends of experimental and calculated values using the (2,10) active space for (a) the axial ZFS parameter $|D|$, and (b) the rhombic ZFS parameter $|E|$. The blue bars correspond to the experimental measurements, and the other bars are for the following electronic structure methods: SA-CASSCF (brown), MS-CASPT2 (green), MS-PDFT(tPBE) (yellow), and HMS-PDFT(tPBE0) (red).

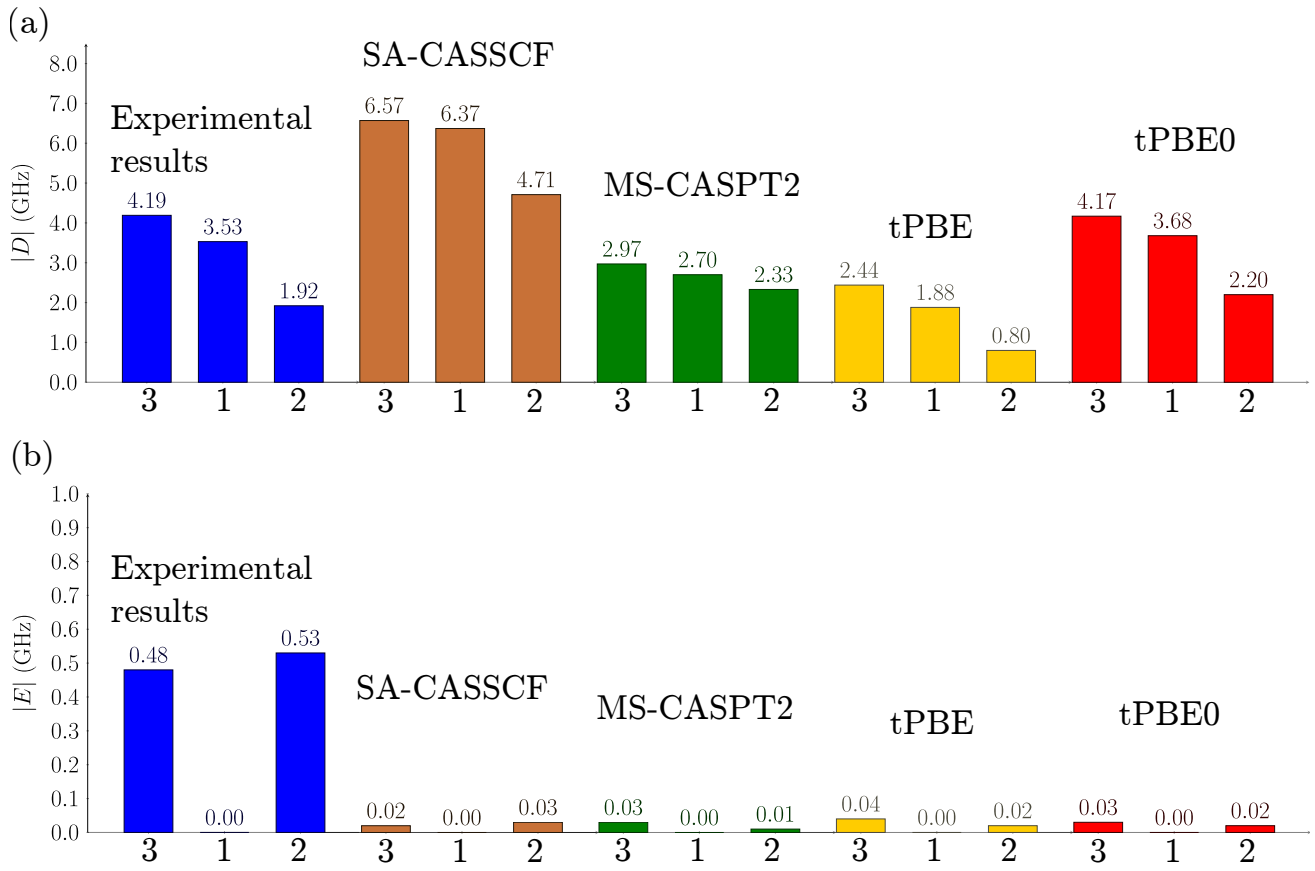

Figure S27: Trends of experimental and calculated values using the (8,8) active space for (a) the axial ZFS parameter $|D|$, and (b) the rhombic ZFS parameter $|E|$. The blue bars correspond to the experimental measurements, and the other bars are for the following electronic structure methods: SA-CASSCF (brown), MS-CASPT2 (green), MS-PDFT(tPBE) (yellow), and HMS-PDFT(tPBE0) (red).

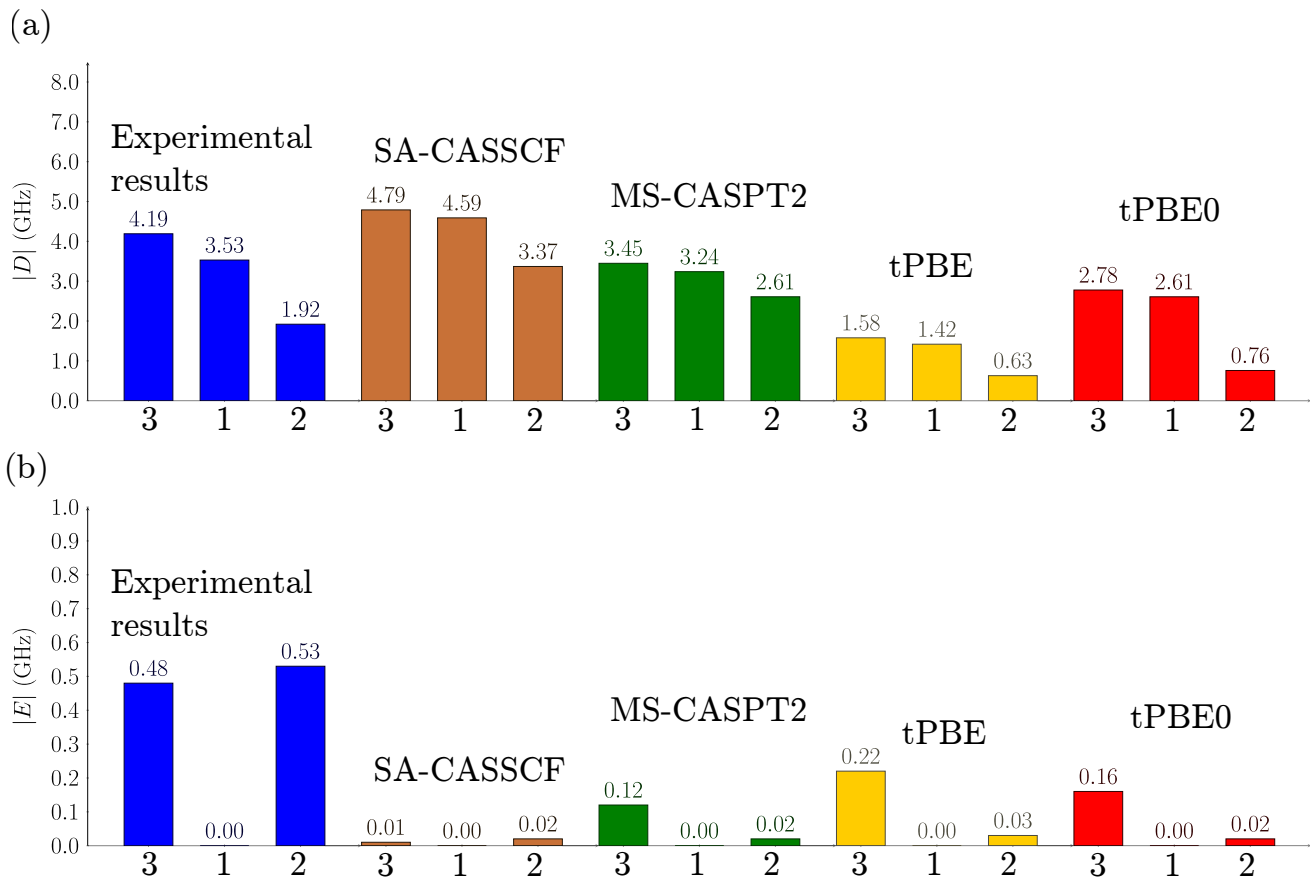

Figure S28: Trends of experimental and calculated values using the (10,15) active space for (a) the axial ZFS parameter $|D|$, and (b) the rhombic ZFS parameter $|E|$. The blue bars correspond to the experimental measurements, and the other bars are for the following electronic structure methods: SA-CASSCF (brown), MS-CASPT2 (green), MS-PDFT(tPBE) (yellow), and HMS-PDFT(tPBE0) (red).

Table S24: Spin-orbit-free energies relative to the ground state of the seven lowest triplet states as calculated with the (2,5) active space at the optimized geometries. The energies were computed with MS-CASPT2 and HMC-PDFT(tPBE0). The values are reported in eV, and cm^{-1} inside the parenthesis.

	3		**1**		**2**	
Method	MS-CASPT2	tPBE0	MS-CASPT2	tPBE0	MS-CASPT2	tPBE0
1	0.000(0.0)	0.000(0.0)	0.000(0.0)	0.000(0.0)	0.000(0.0)	0.000(0.0)
2	2.563(20672.0)	2.277(18365.2)	2.532(20421.9)	2.225(17945.8)	2.641(21301.1)	2.281(18397.5)
3	2.676(21583.4)	2.351(18962.1)	2.709(21849.5)	2.462(19857.4)	2.695(21736.6)	2.326(18760.4)
4	2.729(22010.9)	2.407(19413.8)	2.710(21857.6)	2.462(19857.4)	2.688(21680.2)	2.336(18841.1)
5	3.116(25132.2)	3.065(24720.9)	2.853(23011.0)	2.715(21897.9)	3.091(24930.6)	3.051(24608.0)
6	3.359(27092.1)	3.222(25987.2)	3.622(29213.4)	3.605(29076.3)	3.514(28342.3)	3.197(25785.5)
7	3.463(27931.0)	3.330(26858.2)	3.623(29221.5)	3.605(29076.3)	3.562(28729.5)	3.232(26067.8)

1 eV = 8 065.54 cm^{-1}.

Table S25: Spin-orbit-free energies relative to the ground state of the seven lowest triplet states as calculated with the (2,10) active space at the optimized geometries. The energies were computed with MS-CASPT2 and HMC-PDFT(tPBE0). The values are reported in eV, and cm^{-1} inside the parenthesis.

	3		**1**		**2**	
Method	MS-CASPT2	tPBE0	MS-CASPT2	tPBE0	MS-CASPT2	tPBE0
1	0.000(0.0)	0.000(0.0)	0.000(0.0)	0.000(0.0)	0.000(0.0)	0.000(0.0)
2	2.587(20865.6)	2.292(18486.2)	2.574(20760.7)	2.241(18074.9)	2.666(21502.7)	2.333(18816.9)
3	2.660(21454.3)	2.366(19083.1)	2.738(22083.4)	2.478(19986.4)	2.721(21946.3)	2.379(19187.9)
4	2.745(22139.9)	2.422(19534.7)	2.738(22083.4)	2.478(19986.4)	2.726(21986.7)	2.387(19252.4)
5	3.143(25350.0)	3.068(24745.1)	2.851(22994.9)	2.714(21889.9)	3.101(25011.2)	3.051(24608.0)
6	3.369(27172.8)	3.234(26084.0)	3.644(29390.8)	3.611(29124.7)	3.520(28390.7)	3.216(25938.8)
7	3.463(27931.0)	3.342(26955.0)	3.644(29390.8)	3.611(29124.7)	3.569(28785.9)	3.253(26237.2)

1 eV = 8 065.54 cm^{-1}.

Table S26: Spin-orbit-free energies relative to the ground state of the seven lowest triplet states as calculated with the (8,8) active space at the optimized geometries.The energies were computed with MS-CASPT2 and HMC-PDFT(tPBE0). The values are reported in eV, and cm^{-1} inside the parenthesis.

	3		**1**		**2**	
Method	MS-CASPT2	tPBE0	MS-CASPT2	tPBE0	MS-CASPT2	tPBE0
1	0.000(0.0)	0.000(0.0)	0.000(0.0)	0.000(0.0)	0.000(0.0)	0.000(0.0)
2	2.406(19405.7)	2.332(18808.8)	2.319(18704.0)	2.269(18300.7)	2.440(19679.9)	2.404(19389.6)
3	2.525(20365.5)	2.424(19550.9)	2.538(20470.3)	2.594(20922.0)	2.449(19752.5)	2.443(19704.1)
4	2.515(20284.8)	2.482(20018.7)	2.538(20470.3)	2.595(20930.1)	2.485(20042.9)	2.475(19962.2)
5	2.751(22188.3)	2.842(22922.3)	2.554(20599.4)	2.596(20938.1)	2.762(22277.0)	2.837(22881.9)
6	2.970(23954.7)	2.996(24164.4)	3.166(25535.5)	3.259(26285.6)	2.991(24124.0)	3.012(24293.4)
7	3.093(24946.7)	3.085(24882.2)	3.166(25535.5)	3.259(26285.6)	3.031(24446.7)	3.053(24624.1)

1 eV = 8 065.54 cm^{-1}.

Table S27: Spin-orbit-free energies relative to the ground state of the seven lowest states as calculated with the (10,15) active space at the optimized geometries. The energies were computed with MS-CASPT2 and HMC-PDFT(tPBE0). The values are reported in eV, and cm^{-1} inside the parenthesis.

	3		**1**		**2**	
Method	MS-CASPT2	tPBE0	MS-CASPT2	tPBE0	MS-CASPT2	tPBE0
1	0.000(0.0)	0.000(0.0)	0.000(0.0)	0.000(0.0)	0.000(0.0 (	0.000(0.0)
2	2.406(19405.7)	2.332(18808.8)	2.319(18704.0)	2.269(18300.7)	2.440(19679.9(	2.404(19389.6)
3	2.525(20365.5)	2.424(19550.9)	2.538(20470.3)	2.594(20922.0)	2.449(19752.5(	2.443(19704.1)
4	2.515(20284.8)	2.482(20018.7)	2.538(20470.3)	2.595(20930.1)	2.485(20042.9(	2.475(19962.2)
5	2.751(22188.3)	2.842(22922.3)	2.554(20599.4)	2.596(20938.1)	2.762(22277.0(	2.837(22881.9)
6	2.970(23954.7)	2.996(24164.4)	3.166(25535.5)	3.259(26285.6)	2.991(24124.0(	3.012(24293.4)
7	3.093(24946.7)	3.085(24882.2)	3.166(25535.5)	3.259(26285.6)	3.031(24446.7(	3.053(24624.1)

1 eV = 8 065.54 cm^{-1}.

Optimized Geometries

The following data corresponds to the optimized structures with periodical calculations.

Molecule 1

Cr	0.000000000	0.000000000	0.000000000
C	-1.512325000	0.242037000	1.232610000
C	1.512359000	-0.242037000	1.232614000
C	0.242035000	1.512340000	-1.232644000
C	-0.242008000	-1.512344000	-1.232646000
C	-1.847295000	-0.705409000	2.225921000
C	1.847348000	0.705410000	2.225950000
C	-0.705416000	1.847357000	-2.226000000
C	0.705440000	-1.847374000	-2.226012000
C	-2.871247000	-0.388256000	3.133125000
C	2.871303000	0.388228000	3.133148000
C	-0.388214000	2.871327000	-3.133176000
C	0.388228000	-2.871346000	-3.133183000
C	-2.198202000	1.468925000	1.172491000
C	2.198265000	-1.468936000	1.172517000
C	1.468928000	2.198262000	-1.172562000
C	-1.468906000	-2.198271000	-1.172563000
C	-3.547217000	0.830628000	3.061351000
C	3.547264000	-0.830641000	3.061393000
C	0.830639000	3.547299000	-3.061413000
C	-0.830631000	-3.547308000	-3.061417000
C	-3.217736000	1.763150000	2.075052000

C	3.217779000	-1.763152000	2.075096000
C	1.763132000	3.217796000	-2.075134000
C	-1.763115000	-3.217804000	-2.075134000
C	-1.117588000	-2.017107000	2.355632000
C	1.117618000	2.017100000	2.355634000
C	-2.017108000	1.117620000	-2.355657000
C	2.017133000	-1.117637000	-2.355666000
H	-3.141388000	-1.113549000	3.905304000
H	3.141416000	1.113499000	3.905319000
H	-1.113485000	3.141459000	-3.905325000
H	1.113489000	-3.141476000	-3.905341000
H	-1.927612000	2.201896000	0.411106000
H	1.927666000	-2.201902000	0.411115000
H	2.201893000	1.927648000	-0.411138000
H	-2.201863000	-1.927650000	-0.411131000
H	-4.332739000	1.052059000	3.782093000
H	4.332764000	-1.052075000	3.782121000
H	1.052078000	4.332776000	-3.782129000
H	-1.052076000	-4.332786000	-3.782126000
H	-3.749171000	2.712970000	2.010498000
H	3.749197000	-2.712964000	2.010536000
H	2.712931000	3.749210000	-2.010537000
H	-2.712914000	-3.749201000	-2.010535000
H	-0.656567000	-2.331327000	1.411220000
H	0.656593000	2.331298000	1.411211000
H	-2.331263000	0.656611000	-1.411215000
H	2.331272000	-0.656626000	-1.411222000

H	-1.789644000	-2.817970000	2.690412000
H	1.789646000	2.817970000	2.690408000
H	-2.817972000	1.789638000	-2.690407000
H	2.817997000	-1.789647000	-2.690417000
H	-0.307589000	-1.938919000	3.097397000
H	0.307620000	1.938896000	3.097385000
H	-1.938909000	0.307612000	-3.097383000
H	1.938918000	-0.307629000	-3.097389000

Molecule 2

Cr	0.000000000	0.000000000	0.000000000
C	-2.705519000	-0.434689000	-0.979062000
C	2.705519000	0.434690000	-0.979062000
C	-2.104223000	-2.410950000	-2.877194000
C	2.104223000	2.410951000	-2.877194000
C	-0.859481000	1.351378000	1.166477000
C	0.859481000	-1.351378000	1.166477000
C	-3.421753000	-1.974486000	-2.688826000
C	3.421753000	1.974487000	-2.688826000
C	-0.559014000	2.713926000	0.985864000
C	0.559014000	-2.713925000	0.985864000
C	-1.062452000	-1.835232000	-2.113078000
C	1.062451000	1.835233000	-2.113078000
C	-1.371486000	-0.851753000	-1.148498000
C	1.371487000	0.851754000	-1.148498000
C	-1.754354000	0.954966000	2.183753000

C	1.754353000	-0.954965000	2.183753000
C	-1.810824000	-3.476472000	-3.898184000
C	1.810824000	3.476473000	-3.898184000
C	-2.024628000	-0.495466000	2.476475000
C	2.024628000	0.495467000	2.476475000
C	-3.725498000	-0.989499000	-1.751216000
C	3.725498000	0.989499000	-1.751216000
C	-1.154112000	3.678058000	1.801568000
C	1.154113000	-3.678058000	1.801568000
C	0.351454000	-2.280997000	-2.369014000
C	-0.351454000	2.280998000	-2.369014000
H	-2.949033000	0.337409000	-0.250068000
H	2.949033000	-0.337409000	-0.250068000
H	-4.215610000	-2.401876000	-3.301979000
H	4.215610000	2.401877000	-3.301979000
H	0.147865000	3.025154000	0.215352000
H	-0.147865000	-3.025154000	0.215352000
H	-1.393678000	-4.381131000	-3.428384000
H	1.393678000	4.381131000	-3.428384000
H	-1.070331000	-3.144355000	-4.640623000
H	1.070330000	3.144355000	-4.640623000
H	-2.726935000	-3.756708000	-4.433361000
H	2.726934000	3.756708000	-4.433361000
H	-1.766842000	-1.155257000	1.640778000
H	1.766842000	1.155258000	1.640778000
H	-4.755255000	-0.650897000	-1.629331000
H	4.755255000	0.650897000	-1.629331000

H	-0.936267000	4.735735000	1.661709000
H	0.936267000	-4.735735000	1.661709000
H	0.470463000	-3.364020000	-2.208056000
H	-0.470463000	3.364020000	-2.208056000
H	1.080899000	-1.766091000	-1.734734000
H	-1.080900000	1.766092000	-1.734734000
H	0.639666000	-2.097400000	-3.415866000
H	-0.639667000	2.097401000	-3.415866000
C	-2.370400000	1.936577000	2.994399000
C	2.370399000	-1.936577000	2.994399000
H	-3.072590000	-0.677892000	2.741764000
H	-1.429293000	-0.816654000	3.345601000
H	3.072590000	0.677893000	2.741764000
H	1.429293000	0.816654000	3.345601000
C	-2.043193000	3.284432000	2.798817000
C	2.043194000	-3.284432000	2.798817000
C	-3.357637000	1.553881000	4.059477000
C	3.357637000	-1.553881000	4.059477000
H	-2.494987000	4.030897000	3.453230000
H	2.494987000	-4.030897000	3.453230000
H	-4.215287000	1.012775000	3.631880000
H	-3.739647000	2.438337000	4.581385000
H	-2.913973000	0.882876000	4.808253000
H	2.913973000	-0.882875000	4.808253000
H	3.739647000	-2.438337000	4.581385000
H	4.215286000	-1.012774000	3.631880000

Molecule 3

Cr	0.000000000	0.000000000	0.000000000
C	-1.101538000	1.118807000	-1.191509000
C	0.210792000	-1.794205000	-0.801873000
C	1.750477000	0.878426000	0.244871000
C	-1.690146000	2.347754000	-0.806952000
C	1.040010000	-2.054335000	-1.920561000
C	-0.889700000	-0.178247000	1.758453000
C	1.088468000	-3.356621000	-2.432460000
C	-2.531733000	2.647645000	-3.097646000
C	-2.267456000	-0.470880000	1.908468000
C	-1.258501000	0.673675000	-2.515058000
C	-0.511141000	-2.857522000	-0.234036000
C	-2.390778000	3.083981000	-1.772358000
C	1.847046000	2.237463000	-0.106638000
C	0.363847000	-4.418418000	-1.872264000
C	-0.109938000	0.003851000	2.912655000
C	-2.803122000	-0.566695000	3.200585000
C	2.869932000	0.246064000	0.838242000
C	-0.662228000	-0.097476000	4.189460000
C	-1.600214000	2.868855000	0.602564000
C	-2.023772000	-0.377804000	4.350893000
C	-0.438902000	-4.149479000	-0.758121000
C	-3.176499000	-0.646495000	0.721303000
C	4.105318000	2.370902000	0.773323000
C	2.999586000	2.972931000	0.162867000
C	4.016264000	1.009976000	1.097276000

C	0.463026000	-5.802551000	-2.442457000
C	1.901354000	-0.985955000	-2.537758000
C	2.866701000	-1.220405000	1.172421000
C	5.349971000	3.161740000	1.046537000
C	-2.632826000	-0.440443000	5.721253000
H	-0.827441000	-0.277068000	-2.821179000
H	-1.136361000	-2.682621000	0.640218000
H	-2.827214000	4.043368000	-1.479235000
H	1.012237000	2.733824000	-0.600945000
H	0.952633000	0.227356000	2.824825000
H	-3.866291000	-0.799266000	3.313219000
H	-0.021132000	0.023260000	5.065022000
H	-2.268059000	2.303311000	1.267474000
H	-1.886343000	3.926674000	0.661088000
H	-0.591297000	2.757874000	1.021673000
H	-1.017737000	-4.952085000	-0.295130000
H	-3.519062000	0.328501000	0.342760000
H	-4.065926000	-1.237352000	0.978619000
H	-2.672364000	-1.140345000	-0.118999000
H	3.039907000	4.031458000	-0.098054000
H	4.875745000	0.525090000	1.566504000
H	-0.418284000	-6.397173000	-2.180365000
H	1.343378000	-6.337911000	-2.053548000
H	1.397176000	-0.013355000	-2.601103000
H	2.802408000	-0.819447000	-1.930596000
H	2.064174000	-1.483565000	1.876849000
H	3.817583000	-1.531861000	1.621724000

H	2.702459000	-1.834094000	0.277358000
H	5.883688000	3.394255000	0.112668000
H	6.041704000	2.615498000	1.698565000
H	5.109001000	4.114590000	1.534288000
H	-2.860480000	0.572920000	6.088861000
H	-1.941166000	-0.897426000	6.442209000
H	-3.568526000	-1.014580000	5.722506000
H	1.708460000	-3.551361000	-3.309566000
C	-3.271384000	3.460602000	-4.116230000
C	-1.957062000	1.424241000	-3.458161000
H	0.546352000	-5.784909000	-3.536796000
H	2.234497000	-1.262048000	-3.546693000
H	-4.288077000	3.066296000	-4.256833000
H	-3.359591000	4.509861000	-3.812561000
H	-2.766510000	3.419159000	-5.090749000
H	-2.038256000	1.065234000	-4.486061000

References

(S1) Neese, F. The ORCA program system. WIREs Comput. Mol. Sci. **2012**, 2, 73–78.

(S2) Neese, F. Software Update: The ORCA Program System, Version 4.0. WIREs Comput. Mol. Sci. **2018**, 8, e1327.

(S3) Becke, A. D. Density-Functional Exchange-Energy Approximation with Correct Asymptotic Behavior. Phys. Rev. A **1988**, 38, 3098–3100.

(S4) Lee, C.; Yang, W.; Parr, R. G. Development of the Colle-Salvetti Correlation-Energy Formula into a Functional of the Electron Density. Phys. Rev. B **1988**, 37, 785–789.

(S5) Becke, A. D. Density-functional Thermochemistry. III. The Role of Exact Exchange. J. Chem. Phys. **1993**, 98, 5648–5652.

(S6) Stephens, P. J.; Devlin, F. J.; Chabalowski, M. J., C. F.and Frisch Ab Initio Calculation of Vibrational Absorption and Circular Dichroism Spectra Using Density Functional Force Fields. J. Phys. Chem. **1994**, 98, 11623–11627.

(S7) Perdew, J. P. Density-Functional Approximation for the Correlation Energy of the Inhomogeneous Electron Gas. Phys. Rev. B **1986**, 33, 8822–8824.

(S8) Zhao, Y.; Truhlar, D. G. A new local density functional for main-group thermochemistry, transition metal bonding, thermochemical kinetics, and noncovalent interactions. J. Chem. Phys. **2006**, 125, 194101.

(S9) Zhao, Y.; Truhlar, D. G. The M06 suite of density functionals for main group thermochemistry, thermochemical kinetics, noncovalent interactions, excited states, and transition elements: two new functionals and systematic testing of four M06-class functionals and 12 other functionals. Theor. Chem. Acc. **2008**, 120, 215–241.

(S10) Tao, J. M.; Perdew, J. P.; Staroverov, V. N.; Scuseria, G. E. Climbing the density functional ladder: Nonempirical meta-generalized gradient approximation designed for molecules and solids,. Phys. Rev. Lett. **2003**, 91, 146401.

(S11) Staroverov, V. N.; Scuseria, G. E.; Tao, J.; Perdew, J. P. Comparative Assessment of a New Nonempirical Density Functional: Molecules and Hydrogen-Bonded Complexes. J. Chem. Phys. **2003**, 119, 12129–12137.

(S12) Staroverov, V. N.; Scuseria, G. E.; Tao, J.; Perdew, J. P. Erratum: "Comparative

Assessment of a New Nonempirical Density Functional: Molecules and Hydrogen-Bonded Complexes". J. Chem. Phys. **2004**, 121, 11507.

(S13) Perdew, J. P.; Burke, K.; Ernzerhof, M. Generalized Gradient Approximation Made Simple. Phys. Rev. Lett. **1996**, 77, 3865–3868.

(S14) Ernzerhof, M.; Perdew, J. P. Generalized gradient approximation to the angle- and system-averaged exchange hole,. J. Chem. Phys. **1998**, 109, 3313.

(S15) Adamo, C.; Barone, V. Toward Reliable Density Functional Methods without Adjustable Parameters: The PBE0 Model. J. Chem. Phys. **1999**, 110, 6158–6170.

(S16) Chai, J. D.; Head-Gordon, M. Systematic optimization of long-range corrected hybrid density functionals,. J. Chem. Phys. **2008**, 128, 084106.

(S17) Weigend, F.; Ahlrichs, R. Balanced Basis Sets of Split Valence, Triple Zeta Valence and Quadruple Zeta Valence Quality for H to Rn: Design and Assessment of Accuracy. Phys. Chem. Chem. Phys. **2005**, 7, 3297–3305.

(S18) Neese, F. An Improvement of the Resolution of the Identity Approximation for the Formation of the Coulomb Matrix. J. Comput. Chem. **2003**, 24, 1740–1747.

(S19) Neese, F.; Wennmohs, F.; Hansen, A.; Becker, U. Efficient, Approximate and Parallel Hartree-Fock and Hybrid DFT Calculations. A "Chain-of-Spheres" Algorithm for the Hartree–Fock Exchange. Mov. Front. Quantum Chem. **2009**, 356, 98–109.

(S20) Kossmann, S.; Neese, F. Comparison of Two Efficient Approximate Hartee-Fock Approaches. Chem. Phys. Lett. **2009**, 481, 240–243.

(S21) Kossmann, S.; Neese, F. Efficient Structure Optimization with Second-Order Many-Body Perturbation Theory: The RIJCOSX-MP2 Method. J. Chem. Theory Comput. **2010**, 6, 2325–2338.

(S22) Izsák, R.; Neese, F. An Overlap Fitted Chain of Spheres Exchange Method. J. Chem. Phys. **2011**, 135, 144105.

(S23) Izsák, R.; Neese, F. Speeding up Spin-Component-Scaled Third-Order Pertubation Theory with the Chain of Spheres Approximation: The COSX-SCS-MP3 Method. Mol. Phys. **2013**, 111, 1190–1195.

(S24) Neese, F. Calculation of the Zero-Field Splitting Tensor on the Basis of Hybrid Density Functional and Hartree-Fock Theory. J. Chem. Phys. **2007**, 127, 164112.

(S25) Bayliss, S. L.; Laorenza, D. W.; Mintum, P. J.; Kovos, B. D.; Freedman, D. E.; Awschalom, D. D. Optically addressable molecular spins for quantum information processing. Science **2020**, 370, 1309–1312.